NIH Public Access
Author Manuscript
Hear Res. Author manuscript; available in PMC 2010 August 1.

Published in final edited form as:
Hear Res. 2009 August ; 254(1-2): 1–14. doi:10.1016/j.heares.2009.03.014.

Immunohistochemical distribution of basement membrane proteins in the human inner ear from older subjects

Akira Ishiyama[1,*], **Sarah E Mowry**[1,*], **Ivan A Lopez**[1], and **Gail Ishiyama**[2]

[1]Department of Surgery, Division of Head and Neck, UCLA, Los Angeles, California, USA

[2]Department of Neurology, David Geffen School of Medicine, UCLA, Los Angeles, California, USA

Abstract

The immunolocalization of several basement membrane (BM) proteins was investigated in vestibular endorgans microdissected from temporal bones obtained from subjects with a documented normal auditory and vestibular function (n = 5, average age = 88 years old). Fluorescent immunostaining using antibodies directed at collagen IVα2, nidogen-1, laminin-β2, α-dystroglycan, and tenascin-C was applied to cryosections from human cochlea, cristae ampullares, utricular and saccular maculae. Collagen IVα2, nidogen-1, and laminin-β2 localized to all subepithelial cochlear BMs, Reissner's membrane, strial and spiral ligamental perineural and perivascular BMs, and the spiral limbus. Tenascin-C localized to the basilar membrane and the osseous spiral lamina. α-dystroglycan localized to most cochlear BMs except those in the spiral ligament, basilar membrane and spiral limbus. Collagen IV, nidogen-1, and laminin-β2 localized to the subepithelial BMs of the maculae and cristae ampullares, and the perineural and perivascular BMs within the underlying stroma. The BM underlying the transitional and dark cell region of the cristae ampullares also expressed collagen IV, nidogen-1, and laminin β2. Tenascin-C localized to the subepithelial BMs of the utricular maculae and cristae ampullares, and to calyx-like profiles throughout the vestibular epithelium, but not to the perineural and perivascular BMs. α-dystroglycan colocalized with aquaporin-4 in the basal vestibular supporting cell, and was also expressed in the subepithelial BMs, as well as perivascular and perineural BMs. This study provides the first comprehensive immunolocalization of these ECM proteins in the human inner ear. The validity of the rodent models for inner ear disorders secondary to BM pathologies was confirmed as there is a high degree of conservation of expression of these proteins in the human inner ear. This information is critical to begin to unravel the role that BMs may play in human inner ear physiology and audiovestibular pathologies.

Keywords

collagen; nidogen; laminin; α-dystroglycan; tenascin-C; aging human temporal bone

© 2009 Elsevier B.V. All rights reserved.

Correspondence to: Gail Ishiyama M.D., UCLA Neurology Department, BOX 951769, 3-250 RNRC, Los Angeles, California 90095-1769. 310-825-5910, Fax: 310-206-1513, gishiyama@mednet.ucla.edu.
*equally contributed to the manuscript

Publisher's Disclaimer: This is a PDF file of an unedited manuscript that has been accepted for publication. As a service to our customers we are providing this early version of the manuscript. The manuscript will undergo copyediting, typesetting, and review of the resulting proof before it is published in its final citable form. Please note that during the production process errors may be discovered which could affect the content, and all legal disclaimers that apply to the journal pertain.

NIH-PA Author Manuscript
NIH-PA Author Manuscript
NIH-PA Author Manuscript

NIH-PA Author Manuscript

NIH-PA Author Manuscript

NIH-PA Author Manuscript

1. Introduction

Pathological alterations of the cochlear basement membranes (BMs), particularly of the perivascular stria vascularis BMs, have been the subject of studies in hearing disorders such as Alport's syndrome, presbycusis, aging and animal models of these disorders (Cosgrove et al., 1998; Gratton et al., 2005; Meyer zum Gottesberge and Felix, 2005; Sakaguchi et al., 1997; Zehnder et al., 2005). The BM is a continuous network of extracellular proteins and proteoglycans located at the epithelial and mesenchymal interface of most tissues, the composition of which varies in a tissue-specific manner during development and repair (Erickson and Couchman, 2000). The mammalian BM is approximately 40–100 nm thick and consists of two distinct layers: the lamina densa, an electron dense layer adjacent to the connective tissue and the lamina rara, the layer adjacent to the producing cell (Martinez-Hernandez and Amenta, 1983; Tsuprun and Santi, 2001). Mammalian BMs are primarily composed of collagen IV, nidogen, laminin and heparin sulfate proteoglycans (Erickson and Couchman, 2000; Tsuprun and Santi, 2001). These extracellular matrix (ECM) molecules provide an important structural role and are believed to participate in the regulation of extracellular ion homeostasis and fluid filtration (Eikmans et al., 2003).

BMs are intertwined networks of polymeric laminin and type IV collagen, bridged by non-covalent interactions with nidogens and proteoglycans (Kalluri, 2003). Most of the studies of collagen IV, laminin, and nidogen expression in cochlear BMs have been in rodent species: mouse (Cosgrove et al., 1996; Rodgers et al., 2001; Meyer zum Gottesberge and Felix, 2005), guinea pig (Weinberger et al., 1999; Kalluri et al., 1998; Takahashi and Hokunan, 1992), rat (Satoh et al., 1998) or chinchilla (Tsuprun and Santi, 2001). There are only a few such studies of the vestibular periphery in any mammalian model (Yamashita et al., 1991; Swartz and Santi, 1999), and there are less than a handful of studies that investigate the composition of human cochlear BMs (Zehnder et al., 2005; Yamashita et al., 1991; Kleppel et al., 1989). And while the expression of laminin and collagen II in the human fetal inner ear has been studied (Yamashita et al., 1991; Khetarpal et al., 1994), developmentally-dependent patterns of expression of ECM molecules have been well-documented (Rodgers et al., 2001; Yamashita and Sekitani, 1992; Whitlon et al., 1999). This validates studying the distribution in the adult human. Kleppel et al. (1989) examined the distribution of collagen IV α1 in human inner ear, and Zehnder et al. (2005) conducted studies on collagen IV α1, 3, and 5 in Alport's syndrome. There are no previous studies in the adult human inner ear examining collagen IVα2, nidogen, or laminin-β2 expression. There are even fewer studies examining the expression of the ECM proteins, α-dystroglycan and tenascin-C. All of the prior studies have been in rodents: mouse (Heaney and Schulte, 2003; Whitlon et al., 1999); chinchilla (Swartz and Santi, 1999; Tsuprun and Santi, 1999) and gerbil (Heaney et al., 2002). There are no prior studies of these ECM macromolecules in the human cochlear or vestibular system, and only one prior study of the vestibular system (Swartz and Santi, 1999).

Collagen IV provides the suprastructural foundation of the mammalian BM and is the most abundant mammalian BM protein. Collagen IV consists of seven alpha chains, including two α1 and one α2 chains, in a standard triple helix conformation (Kefalides, 1971, Khoshnoodi et al., 2008). Unlike most collagens, collagen IV, particularly isoforms IVα1 and IVα2, is found exclusively in BMs. Because of the ubiquitous distribution of collagen IVα1 and IVα2 in the mammalian BMs, we investigated the distribution of collagen IVα2 in the human inner ear in this study. Furthermore, there are no prior studies delineating the distribution of collagen IVα2 in the human cochlea and to our knowledge, there is no study of collagen IVα2 in the vestibular periphery of human or any mammalian model.

Laminins are the second most abundant protein of mammalian BMs, providing an important structural component. It had been previously believed that collagen IV served as the scaffolding

NIH-PA Author Manuscript

NIH-PA Author Manuscript

NIH-PA Author Manuscript

upon which a laminin network was placed. However, recent studies have demonstrated that laminin networks serve as the initial template for BM assembly (McKee et al., 2007). Additionally, of importance in the inner ear, laminins likely play a major role in solute and ion transport across the BM (Jarad et al., 2006). The laminins form heterotrimers of α, β and γ chains in a triple helix conformation (Tunggal et al., 2000; Yurchenco and Schittny, 1990). Laminin demonstrates binding sites for cell surface receptors and proteins including nidogen, α-dystroglycan, agrin and other critical BM components (Meyer zum Gottesberge and Felix, 2005), and laminin expression changes with fetal development in all systems (reviewed in Rodgers et al., 2001). Human laminin-β2 deficiency is associated with congenital nephrosis and eye abnormalities (Zenker et al., 2004). In this study, we evaluated the laminin-β2 expression in the adult human inner ear, and compared its expression with that of human fetal inner ear (Yamashita et al., 1991) and with mouse inner ear (Rodgers et al., 2001).

Nidogen is a small protein with three globular regions linked by both flexible and rigid domains. Nidogen binds several other BM proteins, including perlecan, laminin and collagen IV by well-defined, domain-specific interactions (Hohenester and Engel, 2002; Salmivirta et al., 2002). Nidogen acts a bridge between laminin and collagen IV networks in all BMs (Timpl, 1996), and is believed to act as the connecting element for BM assembly. There is one prior study of the distribution of entactin/nidogen in the chinchilla cochlea (Tsuprun and Santi, 2001) and a limited study in the vestibular periphery (Swartz and Santi, 1999). While there are a few studies in animal models, there are no prior studies of nidogen expression in the human inner ear. With regard to domain-specific interactions, nidogen-1 is better studied than nidogen-2 (Kohfeldt et al., 1998), and thus we delineated nidogen-1 expression in the human cochlea and vestibular endorgans.

Dystroglycan is another major component of the subepithelial BM that may play a role in the assembly and homeostasis of the BM (Erickson and Couchman, 2000), and is part of a multiprotein complex that links the ECM to the actin cytoskeleton of muscle fibers (Guadagno and Moukhles, 2004). Dystroglycan is a heterodimer comprised of an α and a β subunit that acts as a cell-surface receptor complex to link extracellular constituents to the cytoskeleton, and the interaction of dystroglycan with laminin is a critical step in the assembly of BMs (Henry and Campbell, 1998). In central nervous system perivascular BMs, dystroglycan co-distributes with Kir4.1, the inward rectifier potassium channel and aquaporin-4 (AQP4) (Guadagno and Moukhles, 2004). We localized AQP4 to basolateral cochlear and vestibular supporting cells of human (Lopez et al., 2007), similar to rat inner ear (Takumi et al., 1998). Aquaporins may play a role in disorders of endolymphatic water homeostasis, such as Ménière's disease (Ishiyama et al., 2006). Dystroglycan expression has been described in the mouse and the developing and senescent gerbil cochlea (Heaney et al., 2002; Heaney and Schulte, 2003). To our knowledge, there are no prior dystroglycan studies in the human or any mammalian vestibular endorgan and no prior studies in the human cochlea. Therefore, we will determine dystroglycan distribution and its colocalization with AQP4 in the human inner ear.

Tenascin-C is an extracellular glycoprotein that is arranged as a hexamer with variable glycosylation. The protein contains amino-terminal heptad repeats, epidermal growth factor-like repeats, fibronectin type III domain repeats, and a carboxyl-terminal fibrinogen-like globular domain (Hsia and Schwarzbauer, 2005; Chiquet-Ehrismann, 2004). Tenascin-C binds to transmembrane cell surface receptors within the ECM (Iyer et al., 2007), proteoglycans (Day et al., 2004) and other ECM components. Tenascin-C has been implicated in several developmental processes, most notably neural morphogenesis (Wehrle and Chiquet, 1990; Warchol and Speck, 2007), wound healing (Alford and Hankenson, 2006), and tumorigenesis (reviewed by Orend, 2005). The expression and distribution of tenascin-C in the cochlea and vestibular endorgans of chinchilla (Swartz and Santi, 1999; Tsuprun and Santi, 1999) and the

NIH-PA Author Manuscript

NIH-PA Author Manuscript

NIH-PA Author Manuscript

developing mouse (Whitlon et al., 1999) has been studied. To our knowledge, there are no prior studies of tenascin-C expression in the auditory or vestibular endorgan in human.

In the present study, we determine the immunohistochemical distribution of collagen IVα2, laminin-β2, nidogen-1, tenascin-C, and α-dystroglycan in the cochlea and vestibular endorgans obtained from subjects with documented normal vestibular and auditory function. To our knowledge, there are no prior studies of these ECM proteins in the adult human auditory or vestibular periphery. Part of this study has been presented in abstract form (Mowry et al., 2008).

2. Materials and methods

2.1 Specimens (Table 1)

The Institutional Review Board (IRB) of UCLA has approved this study. Appropriate informed consent for inclusion in the study was obtained from each temporal bone donor before death. The temporal bone donors in the present study are part of a National Institute of Health funded Human Temporal Bone Consortium for Research Resource Enhancement through the National Institute on Deafness and Other Communication Disorders. Temporal bones were obtained at autopsy from five subjects with a documented history of normal auditory and vestibular function. The patients ranged in age from 84 to 96 years of age (average age = 88 years old). Four subjects were female and one was male. The postmortem time ranged from 3 to 8 hours (Table 1). The vestibular endorgans and cochlea were microdissected from one temporal bone from each donor.

2.2 Temporal bone removal and vestibular endorgans and cochlea microdissection

At autopsy the whole brain, including the brainstem and blood vessels, was removed from the cranial cavity. The 8^{th} cranial nerve and vascular bundle were sectioned outside the internal auditory canal. The temporal bone was then removed as described by Schuknecht (1968) using a bone plug cutter. The bones were then immediately immersed for 16 hours in cold 4% paraformaldehyde in 0.11 M sodium phosphate buffer (PBS), pH 7.4. Thereafter, the fixative was removed by washing with PBS (10 minutes × 3). Temporal bones were placed under a dissecting microscope (Nikon SMZ1500), and using forceps, the muscle, connective tissue and bone surrounding the membranous labyrinth were carefully removed as described previously (Lopez et al., 2005).

2.3 Tissue preparation for immunocytochemistry

The microdissected utricle, saccule, crista and cochlea were immersed in sucrose 30% (in PBS) for 3–5 days, and then in O.C.T. compound (Tissue Tek, Ted Pella, Redding, CA). Before sectioning, the whole vestibular endorgans and cochlea were placed on Teflon embedding molds (Polysciences Inc., Warrington, PA) and properly oriented under the dissecting microscope to obtain longitudinal mid-modiolar sections of cochlea, cross sections of the maculae utricle or saccule and of the cristae ampullares. Twenty-micron-thick serial sections were obtained using a cryostat (Microm-HN505E). Sections were mounted on Superfrost plus slides (Fisher Scientific, Pittsburgh, PA) and stored at −80°C until their use.

2.4 Indirect immunofluorescence

After thawing at room temperature for 10 minutes, tissue sections were incubated at room temperature for 60 minutes with a blocking solution containing 1% bovine serum albumin (BSA) fraction-V (Sigma, St. Louis, MO) and 0.5% Triton X-100 (Sigma) in PBS. At the end of the incubation, the blocking solution was removed and the primary polyclonal or monoclonal antibody against the specific protein was applied. Antibodies to collagen IVα2, nidogen-1,

NIH-PA Author Manuscript

NIH-PA Author Manuscript

NIH-PA Author Manuscript

laminin-β2, α-dystroglycan, tenascin-C and AQP4 were used. Table 2 describes the characteristics of each antibody, dilution and specificity. Primary antibodies were incubated overnight at 4°C in a humid chamber. The secondary antibodies against rabbit or mouse labeled with Alexa 488 or 594 (1:1000, Molecular Probes, Carlsbad, CA) were applied and incubated for two hours at room temperature in the dark. At the end of the incubation, sections were washed with PBS (3 × 10 minutes) and covered with Vectashield mounting media containing DAPI (Vector Labs, Burlingame, CA) to visualize all cell nuclei.

2.5. Fluorescent microscopic observation and documentation

After immunofluorescent processing, tissue sections were viewed and imaged with a Nikon Eclipse E800 fluorescent microscope equipped with RTSlider spot digital camera and Image Pro PlusTM software. To provide unbiased comparisons of the immunofluorescent signal from a particular antibody between each type of specimen, all images were captured using the same camera settings. Images were processed using the Adobe Photoshop™ software program run on a Macintosh iMAC computer.

2.5.1. Quality of microdissected vestibular endorgans obtained from postmortem temporal bones—Table 1 summarizes the quality of immunostaining obtained from the five temporal bones examined. The distribution pattern of immunoreactivity in the tissue from the five temporal bones was similar between specimens for each of the given proteins studied. There was a differential quality of immunoreactivity with a shorter postmortem time associated with a more intense immunofluorescence signal and low background (Table 1). There was no effect of increasing age on the quality of immunoreactivity. The quality of the microdissected endorgan tissue sections was determined by staining with hematoxylin and eosin (Fig 1): the stained horizontal crista ampullaris (Figs 1A-A2), macula utricle (Fig 1B) and cochlea (Fig 1C) are shown. Figures 1A and 1A1 demonstrate the well-preserved crista sensory epithelia, with type I and type II hair cells, supporting cells and stromal cells easily identified. Hair cell stereocilia could also be identified (Fig 1A2). The macula utricle showed good preservation of the sensory epithelia, with mild swelling of calyceal terminals surrounding type I hair cells. Calyceal swelling is an almost unavoidable postmortem artifact (Fig 1B). The cross-section of the cochlea also exhibited good preservation of the organ of Corti, spiral ligament and stria vascularis, as well as the spiral limbus. The tectorial membrane became detached during the microdissection procedure.

3. Results

3.1 BM protein distribution in vestibular endorgans (Table 3)

3.1a Collagen IVα2 immunoreactivity (-IR) (Figure 2)—Collagen IVα2-IR was expressed in the vestibular BMs located underneath the sensory and non-sensory epithelia, including the BMs underlying the transitional epithelia and the dark cell region of the crista ampullaris (Fig 2A). Collagen-IVα2-IR also localized to the BMs surrounding myelinated nerve fibers and blood vessels running throughout the stroma of the crista ampullaris (Fig 2A) and of the maculae of the utricle (Fig 2B) and saccule (Fig 2C). There was a uniform collagen IVα2-IR signal in all regions of the cristae from the planum semilunatum to the central portion of the cristae. The maculae of the utricle (Fig 2B) and saccule (Fig 2C) revealed a similar distribution and intensity of collagen IVα2-IR, distributed within the epithelial BM and the perivascular and perineural BMs.

3.1b Nidogen-IR (Figure 3)—Nidogen-IR was expressed in the crista and maculae in a similar fashion as collagen IVα2-IR: within the BMs underneath the sensory and non-sensory epithelium, including BMs underneath the transitional epithelia and dark cell regions. Nidogen-IR was noted within the BMs surrounding the stromal nerve fibers and blood vessels in the

NIH-PA Author Manuscript

NIH-PA Author Manuscript

NIH-PA Author Manuscript

crista ampullaris (Fig 3A). Nidogen-IR was uniformly distributed in all regions of the crista from the planum semilunatum to the central portion. Nidogen-IR immunolocalization in the maculae utricle (Fig 3B) and saccule (Fig 3C) was similar in distribution to nidogen-IR in the cristae.

3.1c Tenascin-C-IR (Figure 4)—In the crista ampullaris, tenascin-C-IR was revealed in calyx-like profiles throughout the sensory epithelia from the planum semilunatum (Fig 4A) to the central region of the crista (Fig 4B). Tenascin-C-IR was also expressed in the BMs underneath the sensory epithelia, however, in contrast to collagen IVα2 and nidogen, tenascin-C-IR was more prominent in the central portion of the crista (Fig 4A) than in the BMs beneath the sensory epithelia in the planum semilunatum of the crista (Fig 4B). Figure 4A1 and 4B1 shows a high magnification view of these areas to corroborate the regionally determined tenascin-C-IR pattern. The maculae utricle (Fig 4C) and saccule (Fig 4D), demonstrated a similar pattern of tenascin-C-IR immunolocalization as that in the crista in calyx-like structures throughout the sensory epithelia. Tenascin-C-IR in BMs underneath the crista and maculae sensory epithelia was in close apposition with the basolateral membranes of the supporting cells. In contrast to collagen IVα2-IR and nidogen-IR, tenascin-C-IR was not seen in BMs that surround stromal myelinated nerve fibers and blood vessels of the crista and maculae.

3.1d Laminin-β2-IR (Figure 5)—Laminin-β2-IR was localized in all BMs of the crista in a similar fashion as collagen IVα2 and nidogen. Uniform laminin-β2-IR was seen in the BMs underneath the sensory epithelia (Fig 5A). There was a uniform laminin-β2-IR signal in all regions of the crista from the planum semilunatum to the central portion of the crista. Laminin-β2-IR appeared to be more prominent in BM of the transitional epithelia than the BM underlying the sensory epithelia (Fig 5A). The maculae utricle (Fig 5B) and saccule (Figure 5C), displayed a similar laminin-β2-IR pattern. The BMs surrounding the stromal myelinated nerve fibers and blood vessels of the crista ampullaris and maculae utricle and saccule (Figs 5A–C, respectively) also demonstrated laminin-β2-IR.

3.1e α-dystroglycan-IR (Figure 6)—α-dystroglycan-IR was immunolocalized to all of the BMs of the vestibular endorgans in a similar fashion as collagen IVα2, nidogen, and laminin-β2. However, there was a differential regional expression. α-dystroglycan-IR appeared to be more prominent at the central portion of the crista, compared with the peripheral portion of the crista (Fig 6A). This distribution was seen from the planum semilunatum to the central portion of the crista. α-dystroglycan-IR was also less prominent in BMs of the transitional epithelia and perivascular BMs. The maculae utricle (Fig 6B) and saccule (Fig 6C) revealed a similar α-dystroglycan-IR expression as the crista, but without regional variation. α-dystroglycan-IR in the BMs underneath the maculae sensory epithelia was in close apposition with the basolateral membrane of the supporting cells. The BMs that surround the stromal myelinated nerve fibers of the maculae utricle and saccule also exhibited α-dystroglycan-IR (Fig 6B and 6C).

3.1f α-dystroglycan-IR and AQP4-IR colocalization (Figure 7)—α-dystroglycan-IR and AQP4 were co-localized within the basal portion of the sensory epithelia (Fig 7). α-dystroglycan-IR was found in close relation with the basolateral vestibular supporting cells, and localized within the basal pole of cristae supporting cells (Fig 7A), as well as within the epithelial BMs and stromal perineural and perivascular BMs. AQP4 localized to the basolateral portion of the supporting cells (Fig 7A1). Double immunostaining co-localized α-dystroglycan and AQP4 within all the basal vestibular supporting cells (Fig 7A2). α-dystroglycan was expressed without AQP4 co-expression in the epithelial BMs and the perivascular and perineural BMs (Fig 7A2). A similar colocalization and distribution of α-dystroglycan-IR and AQP4-IR was seen in the maculae utricle and saccule (Figs 7B, 7B1, 7B2).

NIH-PA Author Manuscript

NIH-PA Author Manuscript

NIH-PA Author Manuscript

3.2 BM protein distribution in the cochlea (Table 4)

Cochlear BMs are located underneath the supporting cells, epithelial cells of the spiral limbus, basilar membrane, spiral ligament, stria vascularis, Reissner's membrane and surrounding afferent nerve fibers (perineural) and blood vessels (perivascular) of the stria vascularis, spiral ligament and spiral limbus.

3.2a Collagen IVα2-IR (Figure 8A)—Collagen IVα2-IR was present in all cochlear BMs and BMs underneath the epithelial cells with differential concentration. Perivascular and perineural BMs were the most intense, followed by the interdental and outer sulcus cells (Fig 8A). Reissner's membrane and the osseous spiral lamina exhibited collagen IVα2-IR. The perivascular BMs in the spiral ligament and the stria vascularis demonstrated strong collagen IVα2-IR. Collagen IVα2-IR was not seen in the BMs underneath the inner and outer hair cells. The collagen IVα2-IR pattern was similar from the basal to the apical regions of the cochlea.

3.2b Nidogen-IR (Figure 8B)—The distribution of nidogen-IR was similar to that of collagen IVα2-IR (Fig 8B). Nidogen-IR localized to all cochlear BMs and BMs underneath the epithelial cells with differential concentration, similar to collagen IVα2-IR (Fig 8B). Perivascular and perineural BM nidogen-IR was the most intense, followed by the interdental and outer sulcus cells. Reissner's membrane and the osseous spiral lamina were nidogen-IR. Nidogen was expressed strongly in the perivascular BMs in the spiral ligament and the stria vascularis. Nidogen-IR was not seen beneath the organ of Corti. This nidogen-IR pattern was preserved from the basal to the apical portions of the cochlea.

3.2c Tenascin-C-IR (Figure 8C)—Tenascin-C-IR localized to a more discrete pattern than collagen IVα2-IR or nidogen-IR. Tenascin-C-IR was strongly expressed in the basilar membrane underneath the supporting cells in the pars arcuata and pars pectinata (Fig 8C). Tenascin-C-IR was also seen in the basal portion of the Rosenthal canal, and the osseous spiral lamina. There was no discernible regional variation of the tenascin-C-IR pattern from the basal to the apical portions of the cochlea.

3.2d Laminin-β2-IR (Figure 8D)—The distribution of laminin-β2-IR was similar to that of nidogen-IR and collagen IVα2-IR. Laminin-β2-IR was found in BMs underneath epithelial cells in a uniform distribution. However, laminin-β2-IR was more intense in the basilar membrane and Reissner's membrane than nidogen and collagen IV (Fig 8D). Perivascular and perineural laminin-β2-IR was also intense, followed by the interdental and outer sulcus cells. As with nidogen-IR and collagen IVα2-IR, there was no laminin-β2-IR underneath the inner and outer hair cells. This laminin-β2-IR pattern was consistent from the basal to the apical portion of the cochlea.

3.2e α-dystroglycan-IR (Figure 8E)—α-dystroglycan-IR was demonstrated in the BMs underneath epithelial cells in a uniformly throughout all cochlear BMs. However, α-dystroglycan appeared to be less intensely expressed in the basilar membrane (Fig 8E). Perineural α-dystroglycan-IR was also less intense than perivascular immunoreactivity. However, the perivascular BMs of the stria vascularis displayed intense α-dystroglycan-IR. Interdental and outer sulcus cells also showed α-dystroglycan-IR, as well as the outer sulcus cells and cells in the spiral prominence. The basilar membrane demonstrated moderate α-dystroglycan-IR. In contrast to other BM proteins, collagen IV, nidogen and laminin, the spiral ligament did not express α-dystroglycan. Similarly to the other BMs proteins, α-dystroglycan-IR was not observed underneath the inner and outer hair cells. The α-dystroglycan-IR pattern was conserved from the basal to the apical portion of the cochlea.

NIH-PA Author Manuscript

NIH-PA Author Manuscript

NIH-PA Author Manuscript

3.3 Immunohistochemical controls (Figure 9)

Controls—Positive controls for the several BMs antibodies were tested in the cerebellar cortex and cerebral cortex from the same patients, as well as human kidney tissue from normative controls (Fig 9). These sections were subjected to the same protocol as the immunofluorescence protocol of vestibular endorgans and cochlea cryostat sections. For negative controls, the primary antibody was omitted and the immunoreaction was performed as described above.

The immunolocalization of the BMs proteins match previous reports of distribution in human kidney and brain. Figure 9A, shows nidogen-IR in BMs of the human kidney. The distribution is similar to previously published findings in human kidney (Katz et al., 1991). Fig 9A1 shows nidogen-IR in perivascular BMs of the human cerebellar cortex. Fig 9B shows αdystroglycan-IR in the kidney BMs which is similar to previous reports (Vogtländer et al., 2005). Figure 9B1 shows αdystroglycan-IR in perivascular BMs of the human cortex. Collagen IVα2-IR in the kidney BMs is shown in Figure 9C. The distribution is similar to previously published immunohistochemical studies (Lohi et al., 1997; Utsumi et al., 2001). Figure 9C1 shows collagen IVα2-IR in perivascular BMs of the cerebellar cortex. Fig 9D, shows laminin-β2-IR in human kidney BMs as has been previously demonstrated (Virtanen et al., 1995). Tenascin-C-IR in the organ of Corti of mouse (Fig 9E) is similar to previously published (Whitlon et al., 1999). Figure 9F shows AQP4 immunoreactivity in Hensen cells of the human organ of Corti as previously reported (Lopez et al., 2007). All of the negative controls did not demonstrate immunofluorescence within the tissues. As an example, Figure 9G demonstrates the cross-section of the human crista ampullaris immunostained with all the reagents except for the primary antibody, and no specific reaction was observed.

4. Discussion

The mammalian inner ear is rich in BMs which are highly specialized ECM macromolecules that not only provide structural support, but also regulate cellular differentiation, tissue development and repair. Of particular relevance to inner ear physiology, BMs are believed to mediate ionic and water homeostasis. To date, there is little information regarding the normal BM protein distribution in the human inner ear. We determined the immunolocalization of collagen IVα2, nidogen-1, tenascin-C, laminin-β2, and αdystroglycan in the human cochlear and vestibular microdissected endorgans from temporal bones obtained at autopsy.

4.1a Collagen IVα2-IR

Our studies provide the first immunolocalization of the collagen IVα2 chain in the human inner ear, expressed in strial and spiral ligamental perivascular BMs, the spiral limbus, osseous spiral lamina, cochlear BMs and nerve fibers. We confirm the conservation of collagen IVα2 expression in the human cochlea with rodent models. In the mouse, collagen IVα1 and α2 are found in the perineurium of the osseous spiral lamina, the perivascular BMs of the spiral ligament and strial cytoplasm (Cosgrove et al., 1996). In the chinchilla, collagen IVα2, laminin, and entactin codistributed within the spiral limbus, spiral ligament, nerve fibers, strial and spiral ligamental perivascular BMs (Tsuprun and Santi, 2001). Nonspecific antibodies to collagen IV demonstrated a similar distribution in the cochlea of rat (Satoh et al., 1998) and guinea pig (Takahashi and Hokunan, 1992).

Our studies support a colocalization of collagen IVα2 chains with collagen IVα1 in the human cochlea. Collagen IVα1 localized to all cochlear basement membranes, and collagen IV α3 and 5 localized more specifically to the perivascular stria vascularis in normative archival human temporal bones (Zehnder et al., 2005). At the time of the study, collagen IVα2 antibodies were not available. Kleppel et al. (1989) also studied collagen IVα1 distribution in normative human,

NIH-PA Author Manuscript

NIH-PA Author Manuscript

NIH-PA Author Manuscript

and reported a similar distribution, including perivascular and perineural cochlear BMs, spiral limbus, spiral ligament, the pars pectinata of the basilar membrane, and the osseous spiral lamina. Colocalization of collagen IVα1 and α2 chains has been described in the mouse and guinea pig cochlear BMs (Cosgrove et al., 1996; Kalluri et al., 1998; Meyer zum Gottesberge and Felix, 2005). Mouse kidney glomerular BMs also coprecipitated α1 and α2 (Kalluri and Cosgrove, 2000), and it is now widely believed that the six genetically distinct collagen IVα chains assemble into only three heterotrimers: α1α1α2; α3α4α5; α5α5α6 (Khoshnoodi et al., 2008).

We present the first study of collagen IVα2 in the human vestibular periphery, revealing a uniform distribution within the vestibular BMs beneath the sensory and transitional epithelia and within perineural and perivascular BMs. Takahashi and Hokunan (1992) reported a linear staining pattern under the cristae sensory epithelium of the guinea pig for both collagen IV and laminin, similar to our findings however the other vestibular endorgans were not studied. This study demonstrated a similar collagen IVα2 distribution in the human maculae utricle and saccule as in the crista. Collagen IVα2 localized to BMs which demarcate endolymph from perilymph, which would be ideal for mediating ionic and water homeostasis.

An altered expression of collagen IV chains may have pathophysiological significance. Mutations in the genes encoding the collagen IVα3, 4, and 5 have been implicated in the sensorineural hearing loss and glomerulonephritis of Alport's syndrome (Barker et al., 1990). The mouse deficient in the gene for collagen IVα3 serves as a model for Alport's disease. The thickened strial capillary BMs of the Alport's mouse exhibit an increased expression of entactin and collagen IVα1 and 2, and the endothelial cell exhibits swelling and vacuolization (Cosgrove et al., 1998). Thickening of the strial perivascular BMs in Alport's disease has been reported in one post-mortem temporal bone study using rapid-fixation (Weidauer and Arnold, 1976), but not in other temporal bone studies of Alport's disease (Merchant et al., 2004). Further studies of the BM protein expression may reveal BM pathology in other audiovestibular pathologies.

4.1b Nidogen-IR

This study is the first to examine nidogen expression in the human inner ear, localizing to all cochlear BMs in strial and spiral ligamental perivascular BMs, the spiral limbus, osseous spiral lamina, and nerve fibers, similarly to that of collagen IVα2. The expression of nidogen (also called entactin) is conserved in human as entactin expression has been reported in all cochlear BMs in the mouse (Cosgrove et al., 1996) and in the chinchilla with weak immunoreaction in the basilar and Reissner's membrane (Tsuprun and Santi, 2001). Nidogens are a family of highly conserved sulfated glycoproteins that may have a major structural role in BMs during development in tissues undergoing rapid growth or turnover (Ho et al., 2008).

In the human crista ampullaris, utricular and saccular maculae, nidogen localizes to subepithelial and stromal perivascular and perineural BMs, similar to that of collagen IVα2-IR. There is only one prior study showing entactin/nidogen expression in the vestibular periphery, and the only shown photomicrograph is that beneath the sensory neuroepithelium (Swartz and Santi, 1999). To date, there are no studies regarding a specific role for nidogen in the vestibular periphery. It is likely that the close association of nidogen with other BM proteins, including CIV, allows for the formation of stable BMs essential for proper cell-to-cell interaction.

4.1c Tenascin-C-IR

In this first study of tenascin-C expression in the human cochlea, tenascin-C localized to the basilar membrane and the osseous spiral lamina within the cochlea, and osteocytes of the otic

NIH-PA Author Manuscript

NIH-PA Author Manuscript

NIH-PA Author Manuscript

capsule. The expression of tenascin-C in the human cochlea is similar to that of the adult mouse cochlea (Tsuprun and Santi, 1999), and the adult chinchilla (Swartz and Santi, 1999), demonstrating a highly conserved expression. Tenascin-C in the developing mouse is expressed in regions of nerve fiber growth, predominantly in the spiral lamina and the organ of Corti, concomitant with efferent neurite growth (Whitlon et al., 1999). In our study of the adult human cochlea, there was no detectable tenascin-C expression in the organ of Corti. This likely represents developmental changes in expression, as the adult mouse organ of Corti does not express tenascin-C.

In the human vestibular periphery, tenascin-C expression localized to cup-like profiles surrounding the type I hair cells within the crista ampullaris and macula utricle and saccule, as well as the sensory epithelia BMs, with stronger staining in the apical portion of the crista ampullaris. The loss of expression in the planum semilunatum is similar to that in the chinchilla vestibular system (Swartz and Santi, 1999). The tenascin-C distribution in the human auditory and vestibular periphery is highly conserved with rodent models. Our studies also demonstrate a similar tenascin-C expression in all human vestibular endorgans. There is little information about the role of tenascin-C in the inner ear. Healthy avian utricular calyx cells produce tenascin, and this production disappears immediately following injury with streptomycin, but returns as the hair cells repopulate the utricle (Warchol and Speck, 2007). Tenascin-C is found within the developing and diseased kidney, and the maintenance of the glomerular/capillary boundary may be similar to the separation of perilymph and endolymph. An increased tenascin-C expression has been noted in renal pathologies (Okada et al., 1996). Tenascin-C interacts with other ECM proteins that are found within synapses, particularly syndecan (Dityatev et al., 2006), which may explain the presence of tenascin-C at the interface between the type I hair cells and calyx.

4.1d Laminin-β2-IR

This study is the first to examine laminin-β2 expression in the human audiovestibular periphery, localizing within all cochlear BMs, in the spiral limbus, spiral ligament, nerve fibers, strial and spiral ligamental perivascular BMs, similarly to collagen IVα2 and nidogen-1 expression. This study demonstrates a high degree of conservation of the human cochlea with chinchilla (Tsuprun and Santi, 2001) and guinea pig (Weinberger et al., 1999). A similar distribution of laminin in studies using nonspecific laminin antibodies has been documented in the cochlea of rat (Satoh et al., 1998) and the developing human fetus (Yamashita et al., 1991). In the developing mouse, laminin β2 expression was noted in the BM of the perineurium, spiral prominence, strial capillaries, and throughout all cochlear BMs; interestingly, the BM extending from Hensen's cells in the basilar membrane to the external sulcus region did not express laminin-β2 until adulthood, which may indicate a critical role of this area in the hearing mechanism (Rodgers et al., 2001). Of significance, there are continuous changes in laminin subunit expressions from P2 to adulthood in the mouse cochlea, which likely indicates an important role in inner ear development. In that regard, the recent realization that laminin polymers function as the initial template for BM assembly (Li et al., 2005; McKee et al., 2007) is relevant, as it may be the differential expression of laminins that allows for the binding of the cellular receptors such as α-dystroglycan to trigger supramolecular organization (Li et al., 2005). Consequently, an altered laminin expression would likely impact the physiological properties of the BM secondary to changes in the BM assembly.

The present study also provides the first immunolocalization of laminin in the adult human vestibular endorgan. The laminin distribution is similar to that of guinea pig crista ampullaris (Takahashi and Hokunan (1992). The distribution of laminin in the present study was similar to that in the fetal human vestibular system at 11–15 weeks of gestation (Yamashita et al., 1991) except that in our study of the adult, the BMs beneath the sensory crista ampullaris and

NIH-PA Author Manuscript

NIH-PA Author Manuscript

NIH-PA Author Manuscript

the utricular macula demonstrated equal immunoreactivity. In contrast, in the human fetus, the immunoreactivity in the crista was weaker than that in the utricle (Yamashita et al., 1991). A similar developmental differential laminin expression was noted in the developing chick (Yamashita and Sekitani, 1992). The developmental stages of completion of expression of BM components likely reflect that the cristae ampullares are phylogenetically more recent in origin.

Altered laminin expression in the cochlear BMs may be associated with audiovestibular pathologies. Age-related presbycusis in the gerbil model has been associated with a thickening of the BM of strial capillaries, and increased laminin deposition in the strial perivascular BMs (Sakaguchi et al., 1997). The progression of BM thickening in the strial capillary BM has been associated with strial degeneration apparently underlying presbycusis in the senescent gerbil (Schulte and Schmiedt, 1992; Gratton and Schulte, 1995). Because BMs in the inner ear may mediate fluid transport between the endolymph and perilymph (Satoh et al., 1998), an altered expression of laminin in the BM may be associated with dysfunctional ionic homeostatic mechanisms.

4.1e α-Dystroglycan-IR

α-dystroglycan expression localized to the epithelial BMs lining the scala media, including the strial capillaries, Reissner's membrane, the outer sulcus cells and the osseous spiral lamina throughout the adult human cochlea. The localization is conserved with that in the mouse (Heaney and Schulte, 2003) and gerbil cochlea (Heaney et al., 2002). The one noted difference in the expression in adult gerbil (Heaney et al., 2002) and mouse (Heaney and Schulte, 2003) and the adult human (present study) is the lack of α-dystroglycan expression below the organ of Corti in the human. Differences may be secondary to a diminished expression with increased age, post-mortem changes in human specimens, or true species-specific differences. Our study demonstrates a conservation of α-dystroglycan expression in the adult human cochlea, and to our knowledge is the first study of α-dystroglycan in the adult human inner ear.

An age-related decreased expression of dystroglycan has been noted in the strial capillary BMs of the senescent gerbil (Heaney et al., 2002). Notably, the donated temporal bones in our study had an average age of 88 years old. However, the α-dystroglycan staining in the perivascular stria vascularis of our subjects was robust. Of note, all subjects had documented normal hearing, and no presbycusis. Further studies comparing results from this study with α-dystroglycan expression in younger adults, as well as in older adults with presbycusis may reveal an age-related alteration in α-dystroglycan expression.

In this first study of α-dystroglycan in the vestibular periphery, expression was noted in the BMs underneath the sensory epithelia and the stromal perineural BMs in crista and utricular and saccular maculae. The perivascular BMs exhibited less intense α-dystroglycan-IR, in comparison with collagen IV, nidogen-1, and laminin. The decreased perivascular BM expression of α-dystroglycan may be an age-related alteration, as has been noted in senescent gerbil perivascular strial BMs (Heaney et al., 2002). An alteration of α-dystroglycan expression would likely have significant functional implications. We plan to conduct further studies evaluating the expression of BM proteins in younger adult inner ear to evaluate for age-related changes in expression.

4.1f 2 α-dystroglycan-IR and AQP4-IR co-distribution

α-dystroglycan colocalized with AQP4 in the basolateral vestibular supporting cells in human. Previous studies had demonstrated AQP4 localization to the mouse basal vestibular supporting cell in mouse (Takumi et al., 1998) and adult human (Lopez et al., 2007). Of the ECM macromolecules studied in this investigation, only α-dystroglycan localized to the basolateral supporting cells. In the central nervous system the αβ-dystroglycan complex appears on

NIH-PA Author Manuscript

NIH-PA Author Manuscript

NIH-PA Author Manuscript

neurons, glial cells and blood vessels (Milner et al., 2008). Dystroglycan plays a role in filtration in renal podocytes (Vogtländer et al., 2005), and in maintaining the integrity of the blood brain barrier through interactions between astrocytic ECM proteins and the perivascular BMs (Moukhles et al., 2000). α-dystroglycan is believed to be a laminin receptor, involved in ECM assembly (Montanaro et al., 1999). Colocalization studies suggest a role for laminin and the dystroglycan-containing complex in the targeting and stabilizing of Kir4.1 and AQP4 channels in astrocytic cells, for potassium buffering and water homeostasis (Nagelhus et al., 1999; Guadagno and Moukhles, 2004). The colocalization of AQP4 and α-dystroglycan, suggests a similar role in the inner ear.

5. Conclusions

The BM macromolecules, collagen IVα2, laminin-β2, and nidogen-1 colocalized within all human cochlear and vestibular BMs, as well as perivascular and perineural BMs in zones which demarcate endolymph from perilymph, suggestive of BM involvement in the regulation of water and ionic homeostasis. The collagen IVα2 expression in the cochlea was similar to that in rodent models, and also suggests colocalization of collagen IVα2 with collagen IVα1 in human inner ear. The laminin expression in the adult human was similar to that of developing fetal human except that the phylogenetically newer crista BMs had a diminished expression in human fetal, compared with adult. While only very limited studies of nidogen/entactin exist, our studies demonstrate an apparent conservation of expression in human inner ear. This study also provides evidence that the otolithic organs exhibit a similar BM composition to the crista. α-dystroglycan localized to the stria vascularis, the scala media epithelial BMs, and the osseous spiral lamina, similar to its expression in the mouse. In the human vestibular periphery, α-dystroglycan localized to the epithelial BMs and the perineural BMs, but was of diminished expression in vestibular stromal perivascular BMs, which may represent an age-related alteration in expression. α-dystroglycan was the only ECM macromolecule that colocalized with AQP4 in the basolateral vestibular supporting cell. Similar to rodent models, tenascin-C localized to the basilar membrane and osseous spiral lamina, and osteocytes in the otic capsule, and to calyx-shaped profiles in the vestibular neuroepithelium and to the vestibular epithelial BM. In contrast with animal models, the human BM beneath the organ of Corti did not express tenascin-C and α-dystroglycan. This difference may be secondary to age-related alterations, post-mortem changes, antibody differences or true species-specific differences. To the best of our knowledge, this study is the first to delineate the expression of each of these BM and ECM proteins in the adult human auditory and vestibular system, providing valuable information regarding the composition of the normal human inner ear BMs. The distribution of these ECM proteins in the human inner ear was similar to rodent models, where available data exists for comparison, confirming the use of these animal models for inner ear BM pathologies. It is important to note that the average age of the subjects in the present study was 88-years-old, and the findings may represent age-related BM and ECM protein distributions. Our laboratory is currently conducting studies using younger subjects to corroborate the hypothesis that aging is associated with significant alterations in inner ear ECM and BM protein expression.

Abbreviations

BM, basement membrane; ECM, extracellular matrix; IR, immunoreactivity; AQP, Aquaporin.

Acknowledgments

Grant Support: National Institutes of Health Grants, National Institute on Deafness and Other Communication Disorders (NIDCD) DC 008635; DC 005028, DC 005187.

NIH-PA Author Manuscript

NIH-PA Author Manuscript

NIH-PA Author Manuscript

References

Alford AI, Hankenson KD. Matricellular proteins: extracellular modulators of bone development, remodeling and regeneration. Bone 2006;38(6):749–757. [PubMed: 16412713]

Barker DF, Hostikka SL, Zhou J, Chow LT, Oliphant AR, Gerken SC, Gregory MC, Skolnick MH, Atkin CL, Tryggvason K. Identification of mutation in the COL4A5 collagen gene in Alport Syndrome. Science 1990;248(4960):1224–1227. [PubMed: 2349482]

Chiquet-Ehrismann R. Tenascins: molecules in focus. Int. J. Biochem. Cell Biol 2004;36:986–990. [PubMed: 15094113]

Cosgrove D, Samuelson G, Meehan DT, Miller C, McGee J, Walsh EJ, Siegel M. Ultrastructural, physiological, and molecular defects in the inner ear of a gene-knockout mouse model for autosomal Alport syndrome. Hear. Res 1998;121:84–98. [PubMed: 9682811]

Cosgrove D, Samuelson G, Pinnt J. Immunohistochemical localization of basement membrane collagens and associated proteins in the murine cochlea. Hear. Res 1996;97(1–2):54–65. [PubMed: 8844186]

Day JM, Olin AI, Murdoch AD, Canfield A, Sasaki T, Timpl R, Hardingham TE, Asberg A. Alternative splicing in the aggrecan G3 domain influences binding interactions with tenascin-C and other extracellular matrix proteins. J. Biol. Chem 2004;279(13):12511–12518. [PubMed: 14722076]

Dityatev A, Frischknect R, Seiderbecher CI. Extracellular matrix and synaptic functions. Results Probl. Cell Differ 2006;43:69–97. [PubMed: 17068968]

Eikmans M, Baelde JJ, de Heer E, Bruijn JA. Extracellular matrix homeostasis in renal diseases: a genomic approach. J. Pathol 2003;200:526–536. [PubMed: 12845620]

Erickson AC, Couchman JR. Still more complexity in mammalian basement membranes. J. Histochem. Cytochem 2000;48(10):1291–1306. [PubMed: 10990484]

Gratton MA, Rao VH, Meehan DT, Askew C, Cosgrove D. Matrix metalloproteinase dysregulation in the stria vascularis of mice with Alport syndrome: implications for capillary basement membrane pathology. Am. J. Pathol 2005;166(5):1465–1474. [PubMed: 15855646]

Gratton MA, Schulte BA. Alterations in microvasculature are associated with atrophy of the stria vascularis in quiet-aged gerbils. Hear. Res 1995;82:44–52. [PubMed: 7744712]

Guadagno E, Moukhles H. Laminin-induced aggregation of the inwardly rectyfing potassium channel, Kir4.1, and the water permeable channel, AQP4, via a dystroglycan-containing complex in astrocytes. Glia 2004;47:138–149. [PubMed: 15185393]

Heaney DL, Schulte BA. Dystroglycan expression in the mouse cochlea. Hear. Res 2003;177(1–2):12–20. [PubMed: 12618313]

Heaney DL, Schulte BA, Niedzielski AS. Dystroglycan expression in the developing and senescent gerbil cochlea. Hear. Res 2002;174:9–18. [PubMed: 12433392]

Henry MD, Campbell KP. A role for dystroglycan in basement membrane assembly. Cell 1998;95:859–870. [PubMed: 9865703]

Ho M, Bose K, Mokkapati S, Nischt R, Smyth N. Nidogens-extracellular matrix linker molecules. Microscopy Res. and Tech 2008;71:387–395.

Hohenester E, Engel J. Domain structure and organization in extracellular matrix proteins. Matrix Biology 2002;21(2):115–128. [PubMed: 11852228]

Hsia HC, Schwarzbauer JE. Meet the tenascins: multifunctional and mysterious. J. Biol. Chem 2005;280 (29):26641–26644. [PubMed: 15932878]

Ishiyama G, Lopez IA, Ishiyama A. Aquaporins and Meniere's disease. Curr Opin. Otolaryngol. Head Neck Surg 2006;14(5):332–336. [PubMed: 16974147]

Iyer AK, Tran KT, Borysenko CW, Cascio M, Camacho CJ, Blair HC, Bahar I, Wells A. Tenascin cytotactin epidermal growth factor-like repeat binds epidermal growth factor receptor with low affinity. J. Cell Physiol 2007;211(3):748–758. [PubMed: 17311283]

Jarad G, Cunningham J, Shaw AS, Miner JH. Proteinuria precedes podocyte abnormalities in Lamba2−/− mice, implicating the glomerular basement membrane as an albumin barrier. J. Clin. Invest 2006;116(8):2272–2279. [PubMed: 16886065]

Kalluri R. Basement membranes: structure, assembly and role in tumor angiogenesis. Nat. Rev. Cancer 2003;3:422–433. [PubMed: 12778132]

NIH-PA Author Manuscript

NIH-PA Author Manuscript

NIH-PA Author Manuscript

Kalluri R, Cosgrove D. Assembly of type IV collagen. J. Biol. Chem 2000;275(17):12719–12724. [PubMed: 10777566]

Kalluri R, Gattone VH 2nd, Hudson BG. Identification and localization of type IV collagen chains in the inner ear cochlea. Connect Tissue Res 1998;37(1–2):143–150. [PubMed: 9643653]

Katz A, Fish AJ, Kleppel MM, Hagen SG, Micahel AF, Butkowski RJ. Renal entactin (nidogen): isolation, characterization and tissue distribution. Kidney Int 1991;40(4):643–652. [PubMed: 1745013]

Kefalides NA. Isolation of a collagen from basement membranes containing three identical chains. Biochem. Biophys. Res. Commun 1971;45(1):226–234. [PubMed: 4946405]

Khetarpal U, Robertson NG, Yoo TJ, Morton CC. Expression and localization of COL2A1 mRNA and type II collagen in human fetal cochlea. Hear. Res 1994;79:59–73. [PubMed: 7806485]

Khoshnoodi J, Pedchenko V, Hudson BG. Mammalian collagen IV. Microscopy Res. and Techn 2008;71:357–370.

Kleppel MM, Santi PA, Cameron JD, Wieslander J, Michael AF. Human tissue distribution of novel basement membrane collagen. Am. J. Pathol 1989;134(4):813–825. [PubMed: 2650557]

Kohfeldt E, Sasaki T, Gohring W, Timpl R. Nidogen-2: a new basement membrane protein with diverse binding properties. J. Mol. Biol 1998;282(1):99–109. [PubMed: 9733643]

Li S, Liquari P, McKee KK, Harrison D, Patel R, Lee S, Yurchenco PD. Laminin-sulfatide binding initiates basement membrane assembly and enables receptor signaling in Schwann cells and fibroblasts. J. Cell Biol 2005;169(1):179–189. [PubMed: 15824137]

Lohi J, Korhonen M, Leivo I, Kangas L, Tani T, Kalluri R, Miner JH, Lehto V-P, Virtanen I. Expression of type IV collagen α–α6 polypeptides in normal and developing human kidney and in renal cell carcinomas and oncocytomas. Int. J. Cancer 1997;72:43–49. [PubMed: 9212221]

Lopez IA, Ishiyama G, Lee M, Baloh RW, Ishiyama A. Immunohistochemical localization of aquaporins in the human inner ear. Cell Tissue Res 2007;328(3):453–460. [PubMed: 17318586]

Lopez I, Ishiyama G, Tang Y, Frank M, Baloh RW, Ishiyama A. Estimation of the number of nerve fibers in the human vestibular endorgans using unbiased stereology and immunohistochemistry. J. Neurosci. Methods 2005;145(1–2):37–46. [PubMed: 15922024]

Martinez-Hernandez A, Amenta PS. The basement membrane in pathology. Lab. Invest 1983;48(6):656–677. [PubMed: 6222217]

Merchant SN, Burgess BJ, Adams JC, Kashtan CE, Gregory MC, Santi PA, Colvin R, Collins B, Nadol JB Jr. Temporal bone histopathology in Alport syndrome. Laryngoscope 2004;114:1609–1618. [PubMed: 15475791]

Meyer zum Gottesberge AM, Felix H. Abnormal basement membrane in the inner ear and the kidney of the Mpv17−/− mouse strain: ultrastructural and immunohistochemical investigations. Histochem. Cell Biol 2005;124(6):507–516. [PubMed: 16041630]

McKee KK, Harrison D, Capizzi S, Yurchenco PD. Role of laminin terminal globular domains in basement membrane assembly. J. Biol. Chem 2007;282(29):21437–21447. [PubMed: 17517882]

Milner R, Hung S, Wang X, Spatz M, del Zoppo GJ. The rapid decrease in astrocyte-associated dystroglycan expression by focal cerebral ischemia is protease-dependent. J. Cereb. Blood Flow Metab 2008;28(4):812–823. [PubMed: 18030304]

Montanaro F, Lindenbaum M, Carbonetto S. Alpha-dystroglycan is a laminin receptor involved in extracellular matrix assembly of myotubules and muscle cell viability. J. Cell Biol 1999;145:1325–1340. [PubMed: 10366602]

Mowry, S.; López, IA.; Ishiyama, A.; Ishiyama, G. Immunolocalization of basement membrane proteins in human vestibular endorgans in Meniere's disease, acoustic neuroma and normal. 31st Midwinter Meeting; Association Research in Otolaryngology (ARO); 2008. Abstract 958.

Moukhles H, Roque R, Carbonetto S. Alpha-dystroglycan isoforms are differentially distributed in adult rat retina. J. Comp. Neurol 2000;420:182–194. [PubMed: 10753306]

Nagelhus EA, Horio Y, Inanobe A, Fujita A, Haug FM, Nielsen S, Kurachi Y, Ottersen OP. Immunogold evidence suggests that coupling of K+ siphoning and water transport in rat retinal Müller cells is mediated by a coenrichment of Kir4.1 and AQP4 in specific membrane domains. Glia 1999;26:47–54. [PubMed: 10088671]

Okada M, Takemura T, Murakami K, Hino S, Yoshioka K. Expression of tenascin in normal and diseased human kidneys. Nippon Jinzo Gakkai Shi 1996;38(5):213–219. [PubMed: 8699611]

NIH-PA Author Manuscript

NIH-PA Author Manuscript

NIH-PA Author Manuscript

Orend G. Potential oncogenic action of tenascin-C in tumorigenesis. Int. J. Biochem. Cell Biol 2005;37 (5):1066–1083. [PubMed: 15743679]

Rodgers KD, Barritt L, Miner JH, Cosgrove D. The laminins in the murine inner ear: developmental transitions and expression in cochlear basement membranes. Hear. Res 2001;158:39–50. [PubMed: 11506935]

Sakaguchi N, Spicer SS, Thomopoulos GN, Schulte BA. Increased laminin deposition in capillaries of the stria vascularis of quiet-aged gerbils. Hear. Res 1997;105(1–2):44–56. [PubMed: 9083803]

Salmivirta K, Talts JF, Olsson M, Sasaki T, Timpl R, Ekblom P. Binding of mouse nidogen-2 to basement membrane components and cells and its expression in embryonic and adult tissues suggest complementary functions of the two nidogens. Experimental Cell Res 2002;279:188–201.

Satoh H, Kawasaki K, Kihara I, Nakano Y. Importance of type IV collagen, laminin, and heparan sulfate proteoglycan in the regulation of labyrinthine fluid in the rat cochlear duct. Eur. Arch. Otorhinolaryngol 1998;255(6):285–288. [PubMed: 9693922]

Schuknecht HF. Temporal bone removal at autopsy. Preparation and uses. Arch. Otolaryngol 1968;87 (2):129–137. [PubMed: 4865202]

Schulte BA, Schmiedt RA. Lateral wall NaKATPase and endocochlear potentials decline with age in quiet-reared animals. Hear. Res 1992;61:35–46. [PubMed: 1326507]

Swartz DJ, Santi PA. Immunolocalization of tenascin in the chinchilla inner ear. Hear. Res 1999;130(1–2):108–114. [PubMed: 10320102]

Takahashi M, Hokunan K. Localization of type IV collagen and laminin in the guinea pig inner ear. Ann. Otol. Rhinol. Laryngol. Suppl 1992;157:58–62. [PubMed: 1416655]

Takumi Y, Nagelhus EA, Eidat J, Matsubara A, Usami S, Shinkawa H, Nielsen S, Ottersen OP. Select types of supporting cells in the inner ear express aquaporin-4 water channel protein. Eur. J. Neurosci 1998;10(12):3584–3595. [PubMed: 9875338]

Timpl R. Macromolecular organization of basement membranes. Curr. Opin. Cell Biol 1996;8(5):618–624. [PubMed: 8939648]

Tsuprun V, Santi P. Ultrastructure and immunohistochemical identification of the extracellular matrix of the chinchilla cochlea. Hear. Res 1999;129:35–49. [PubMed: 10190750]

Tsuprun V, Santi P. Proteoglycan arrays in the cochlear basement membrane. Hear. Res 2001;157(1–2): 65–76. [PubMed: 11470186]

Tunggal P, Smyth N, Paulsson M, Ott MC. Laminins: structure and genetic regulation. Microsc. Res. Tech 2000;51(3):214–227. [PubMed: 11054872]

Utsumi K, Shimizu A, Yamato M, Tohimbara T, Nakajima I, Adachi E, Fuchinoue S, Sawada T. Alteration of collagen IV in acutely deteriorated renal allografts. Transplantation 2001;71(12):1757–1765. [PubMed: 11455255]

Virtanen I, Laitinen L, Korhonen M. Differential expression of laminin polypeptides in developing and adult human kidney. J. Histochem. Cytochem 1995;43(6):621–628. [PubMed: 7769233]

Vogtländer NP, Dijkman H, Bakker MA, Campbell KP, van der Vlag J, Berden JH. Localization of alpha-dystroglycan on the podocyte: from top to toe. J. Histochem. Cytochem 2005;53(11):1345–1353. [PubMed: 15956031]

Warchol ME, Speck JD. Expression of GATA3 and tenascin in the avian vestibular maculae: normative patterns and changes during sensory regeneration. J. Comp. Neurol 2007;500(4):646–657. [PubMed: 17154269]

Wehrle B, Chiquet M. Tenascin is accumulated along developing peripheral nerves and allows neurite outgrowth in vitro. Development 1990;110:401–415. [PubMed: 1723942]

Weinberger DG, ten Cate W-C, Lautermann J, Baethmann M. Localization of laminin isoforms in the guinea pig cochlea. Laryngoscope 1999;109:2001–2004. [PubMed: 10591363]

Whitlon DS, Zhang X, Kusakabe M. Tenascin C in the cochlea of the developing mouse. J. Comp. Neurol 1999;4006(3):361–374. [PubMed: 10102501]

Weidauer H, Arnold W. Strukturelle Veranderungen am Hororgan beim Alport Syndrome. Z. Laryngol. Rhinol. Otol 1976;55:6–16.

Yamashita H, Bagger-Sjöbäck D, Wersäll J. The presence of laminin in the fetal human inner ear. Eur. Arch. Otorhinolaryngol 1991;248(8):479–482. [PubMed: 1768411]

NIH-PA Author Manuscript

NIH-PA Author Manuscript

NIH-PA Author Manuscript

Yamashita H, Sekitani T. Laminin in the endolymphatic sac and vestibular endorgans of developing chick embryos. Acta Otolaryngol. Suppl 1992;493:31–36. [PubMed: 1636420]

Yurchenco PD, Schittny JC. Molecular architecture of basement membranes. FASEB J 1990;4(6):1577–1590. [PubMed: 2180767]

Zehnder A, Adams J, Santi P, Kristiansen AG, Wacharasindhu D, Mann S, Kalluri R, Gregory MC, Kashtan CE, Merchant SN. Distribution of type IV collagen in the cochlea in Alport's syndrome. Arch. Otolaryngol. Head Neck Surg 2005;131(11):1007–1013. [PubMed: 16301374]

Zenker M, Aigner T, Wendler O, Tralau T, Muntefering H, Fenski R, Pitz S, Schumacher V, Royer-Pokora B, Wuhl E, Cochat P, Bouvier R, Kraus C, Mark K, Madion H, Dotsch J, Rascher W, Maruniak-Chudek I, Lennert T, Neumann LM, Reis A. Human laminin beta 2 deficiency causes congenital nephrosis with mesangial sclerosis and distinct eye abnormalities. Hum. Mol. Genet 2004;13(21):2625–2632. [PubMed: 15367484]

NIH-PA Author Manuscript
NIH-PA Author Manuscript
NIH-PA Author Manuscript

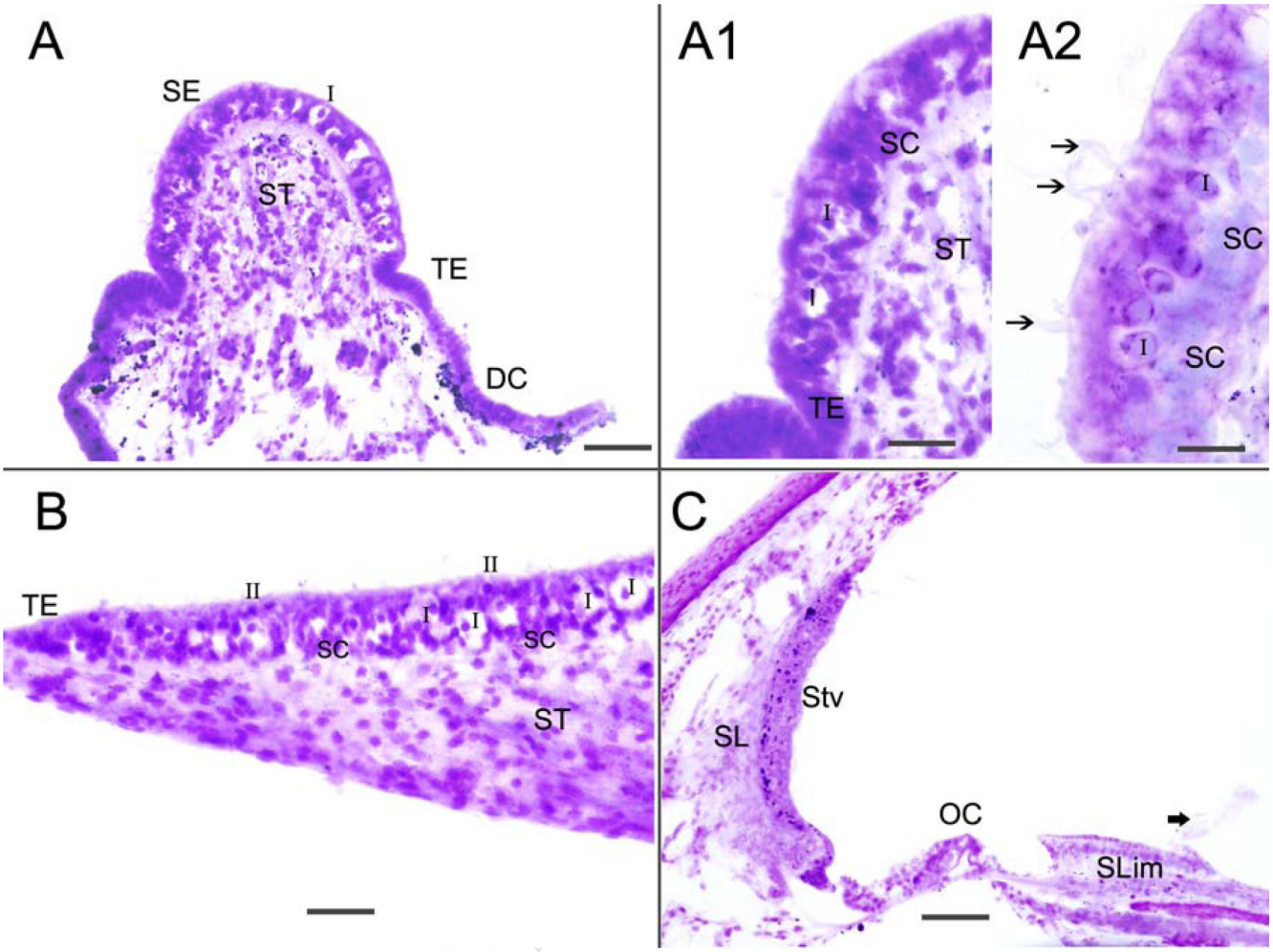

Fig 1.

Hematoxylin and eosin stained frozen section of the crista ampullaris (Fig 1A-A2), macula utricle (Fig 1B) and cochlea (Fig 1C). Fig 1A shows the crista sensory epithelia (SE), the transitional epithelia (TE), the dark cell area (DC) and the stroma tissue (ST). Fig 1A1 and 1A2 are higher magnification views of the cristae. The sensory epithelia is well-preserved and type I (I) and type II (II) hair cells, as well as supporting cells (SC), and cells in the stroma (ST) are easily identified. Hair cell stereocilia can be seen (arrowheads). Fig 1B shows the macula utricle which exhibits good preservation of the sensory epithelia hair cells and supporting cells, with mild swelling of calyceal terminals that surround type I hair cells (I). Figure 1C is a cross-section of the cochlea; there is good preservation of the organ of Corti (OC), spiral ligament (SL) and stria vascularis (Stv) as well as the spiral limbus (Slim). In this specimen, the tectorial membrane and Reissner's membrane had become detached during microdissection (thick arrowhead). Magnification bar is 100 μm for (A) and (C), 50 μm for (A1), 20 μm for (A1), 60 μm for (B).

NIH-PA Author Manuscript
NIH-PA Author Manuscript
NIH-PA Author Manuscript

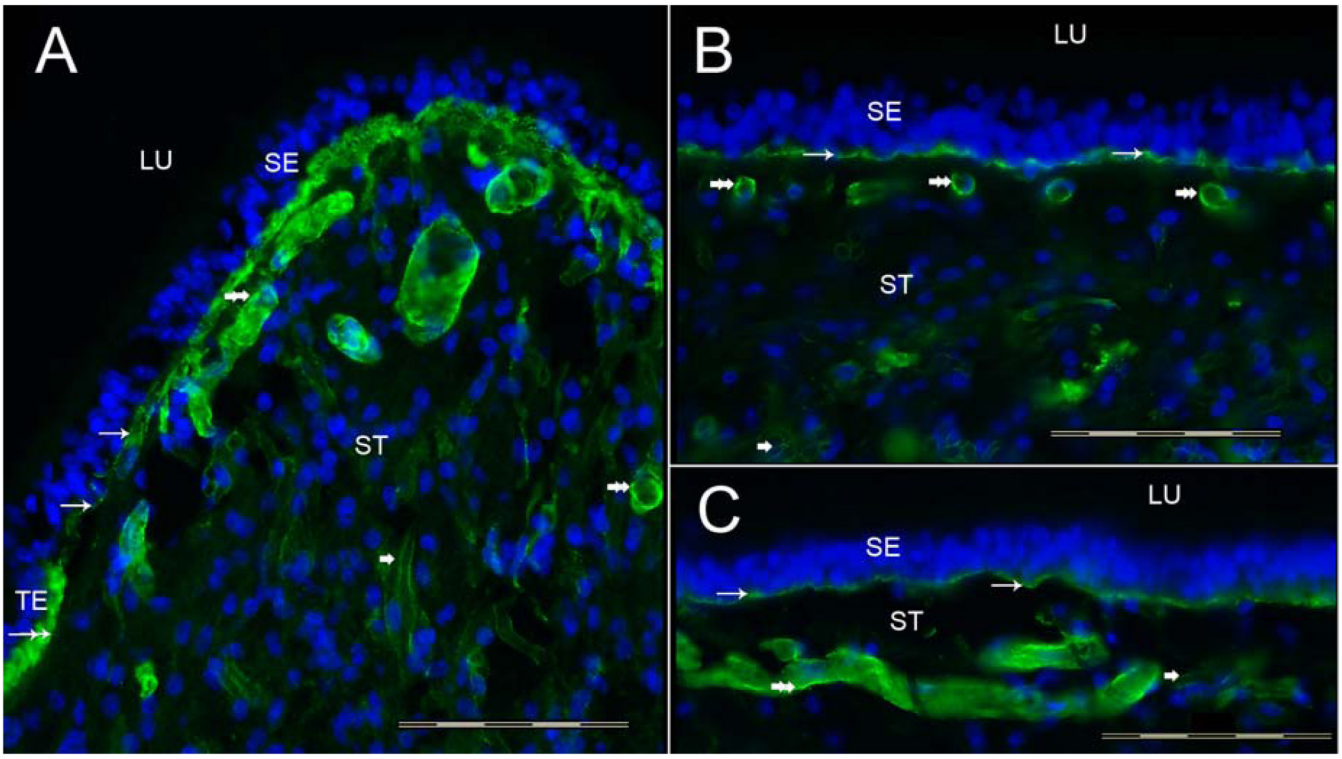

Fig 2.

Collagen IVα2 immunoreactivity (-IR) in the human vestibular endorgans. Fig 2A shows a cross-section of the crista ampullaris, close to the central region. Collagen IVα2-IR (green color) was seen within the BM underneath the sensory epithelia (SE) (thin arrows). The BM underneath the transitional epithelia (TE) also displayed collagen IVα2-IR (double arrow). The perivascular BMs within the underlying stroma (ST) were collagen IVα2-IR (double arrowheads). The perineural BMs beneath the epithelia and within the underlying ST also exhibited collagen IVα2-IR (single arrowhead). The macula utricle (Fig 2B) and macula saccule (Fig 2C) showed a similar collagen IVα2-IR pattern. BMs that surround stromal myelinated nerve fibers (arrowhead) and blood vessels (double arrowhead) of the maculae utricle and saccule were also collagen IVα2-IR. DAPI (blue color) identifies cell nuclei. LU: Lumen. Magnification bar is 200 μm for all figures.

NIH-PA Author Manuscript
NIH-PA Author Manuscript
NIH-PA Author Manuscript

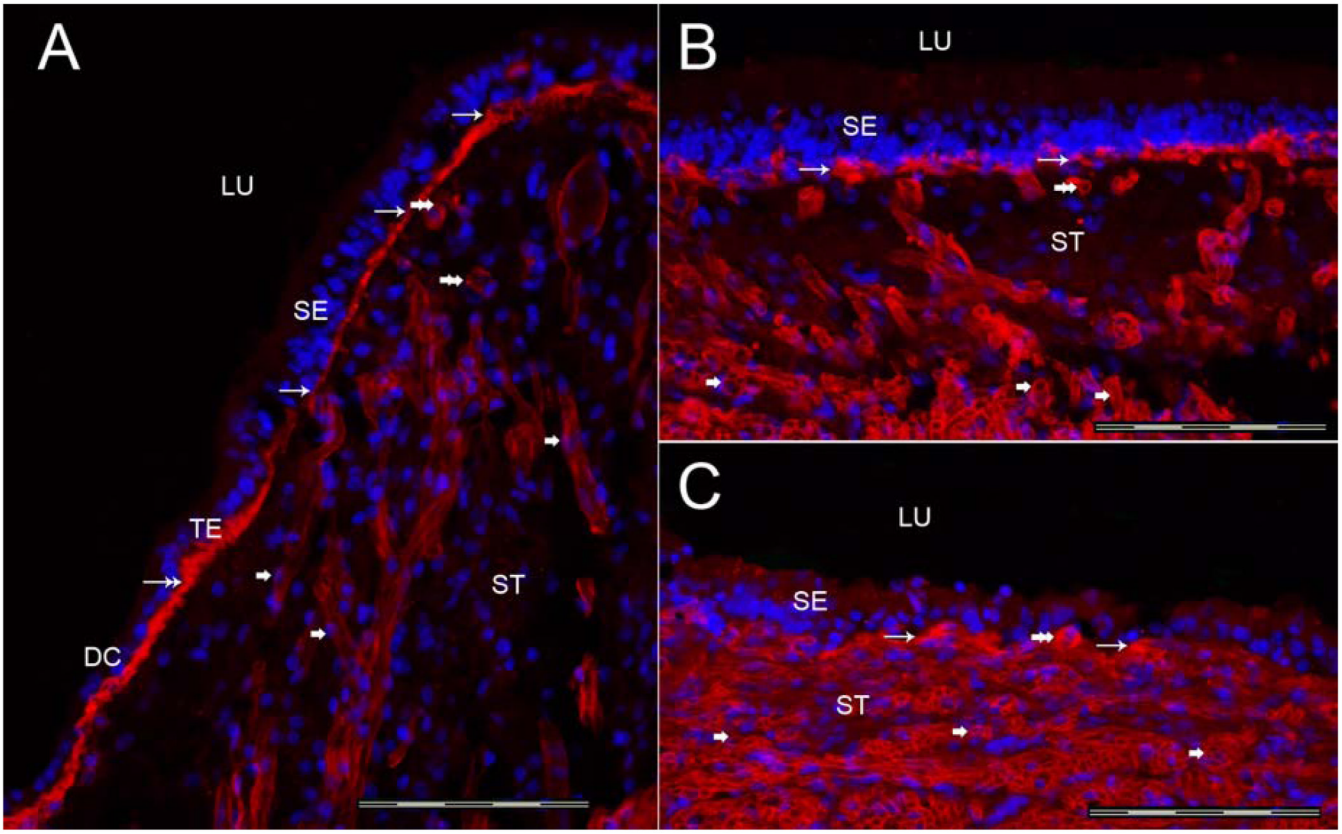

Fig 3.

Nidogen-IR Fig 3A shows a cross-section of the crista ampullaris, close to the central region. Nidogen-IR (red color) was expressed within the BMs underneath the sensory epithelia (SE) (thin arrows). The BMs underlying the transitional epithelia (TE) and dark cells (DC) also exhibited nidogen-IR (double arrow). The perivascular BMs within the underlying stroma expressed nidogen-IR (double arrowhead), and the perineural BMs within the underlying stroma (ST) also demonstrated nidogen-IR (single arrowhead). The distribution of nidogen-IR in the macula utricle (Fig 3B) and macula saccule (Fig 3C) was similar to nidogen-IR within the cristae sensory epithelia. BMs that surround stromal myelinated nerve fibers and blood vessels of the macula utricle and saccule were also nidogen-IR. DAPI (blue color) identifies cell nuclei. Magnification bar is 200 μm for all figures.

NIH-PA Author Manuscript
NIH-PA Author Manuscript
NIH-PA Author Manuscript

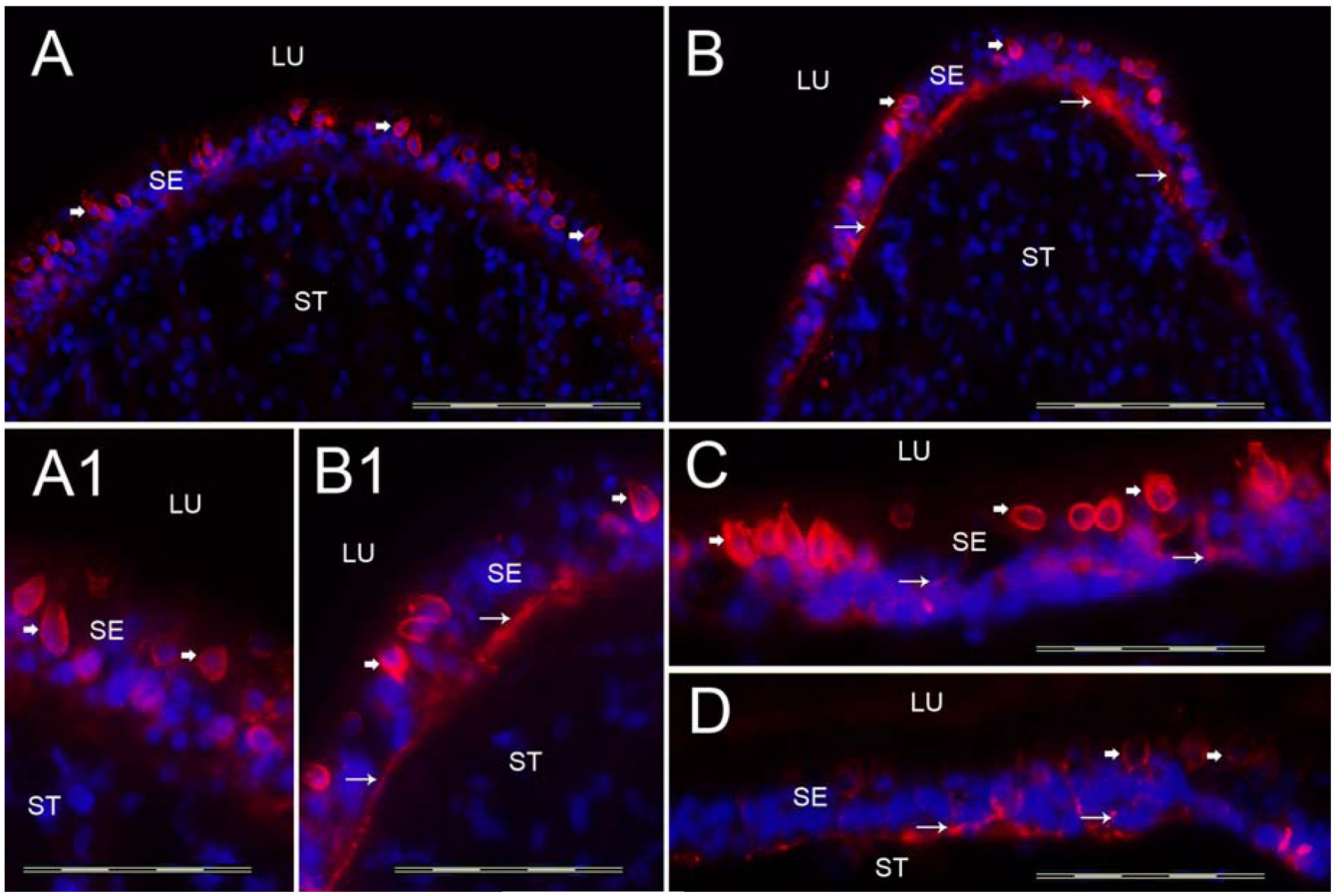

Fig 4.

Tenascin-C-IR. Fig 4A shows a cross-section of the crista ampullaris at the planum semilunatum. Fig 4B shows tenascin-C-IR at the central region of the crista ampullaris. Tenascin-C-IR (red color) was found in calyx-like profiles (arrowheads) throughout the SE and also in BM underneath the SE (arrows). Tenascin-C-IR was more prominent in the central portion of the crista (Fig 4B) than in the BMs underneath the SE in the planum semilunatum of the crista (Fig 4A). Figure 4A1 and 4B1 is a high magnification view (from Fig 4A and 4B) of these areas to demonstrate the tenascin-C-IR pattern. The macula utricle (Fig 4C) and the macula saccule (Fig 4D) exhibited similarly tenascin-C-IR in calyx-like structures (arrowheads) and within the BMs underneath the SE (arrows). DAPI (blue color) identifies cell nuclei. Magnification bar is 200μm for Fig A, B, C and D; 50 μm for fig A1, B1.

NIH-PA Author Manuscript

NIH-PA Author Manuscript

NIH-PA Author Manuscript

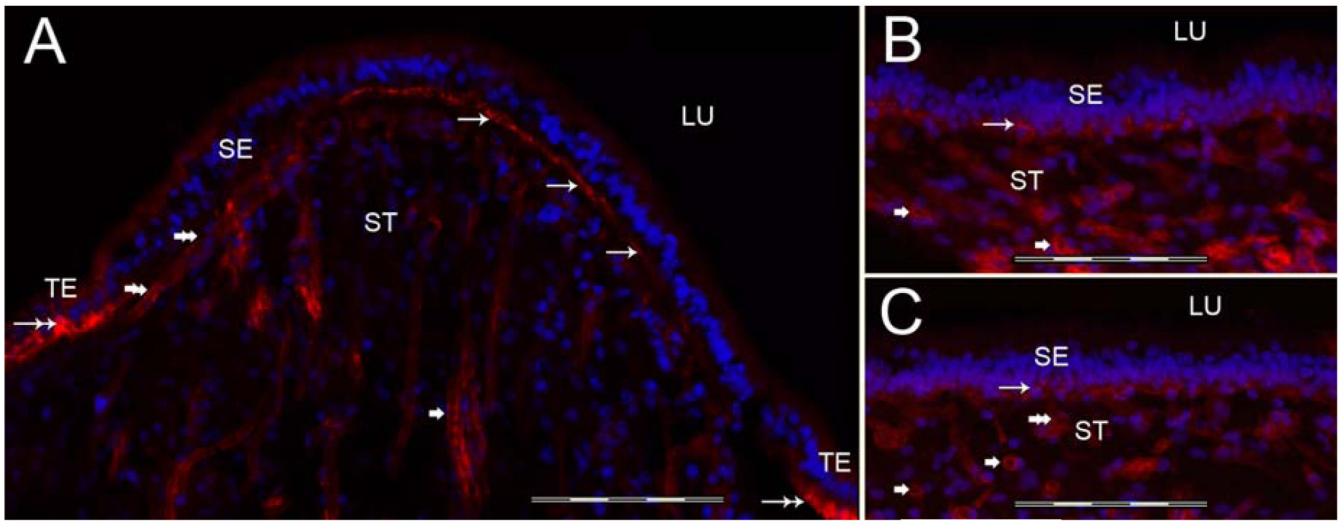

Fig 5.

Laminin-β2-IR. Fig 5A shows Laminin-β2-IR in a cross-section of the crista ampullaris, close to the planum semilunatum. Laminin-β2-IR was seen within the BMs underneath the sensory epithelia (SE) (thin arrows). Transitional epithelia (TE) BMs also demonstrated laminin-β2-IR (double arrows). The maculae utricle (Fig 5B) and saccule (Figure 5C) exhibited a similar laminin-β2-IR expression distribution. Laminin-β2-IR was found in the BMs underneath the maculae SE. The BMs that surround stromal myelinated nerve fibers (arrowheads) and blood vessels (double arrowheads) also expressed laminin-β2 in the cristae ampullares, utricular and saccular maculae. DAPI (blue color) identifies cell nuclei. Magnification bar is 200 μm for all figures.

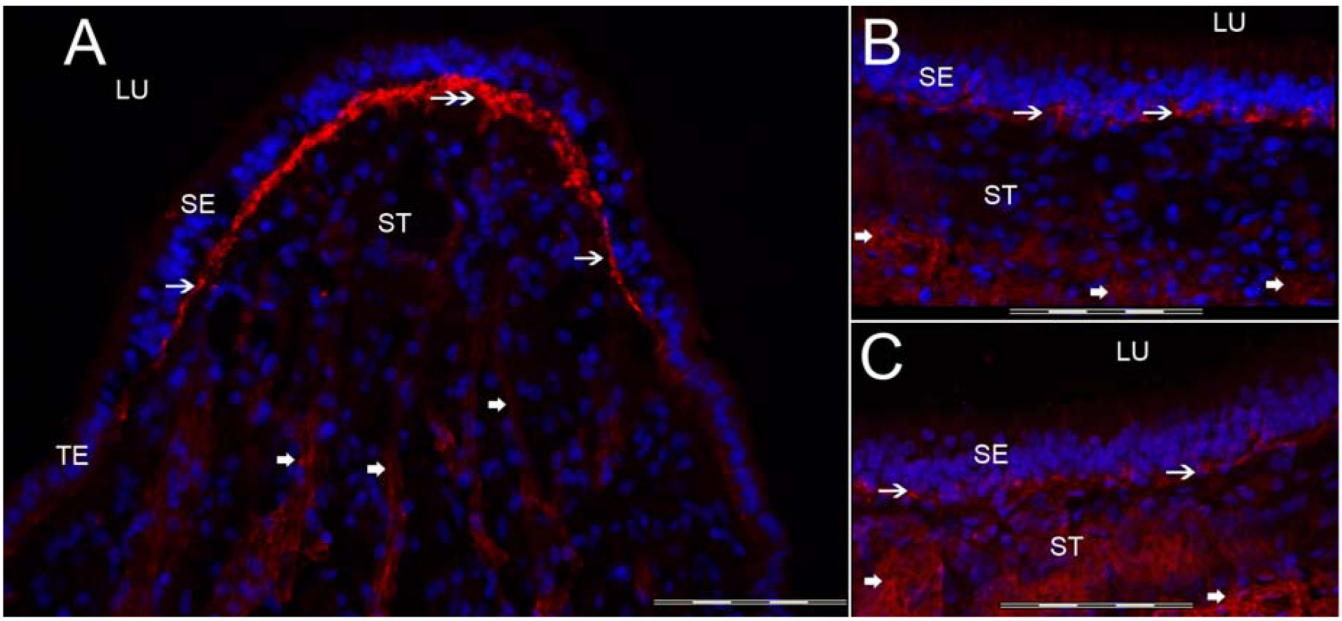

Fig 6.

α-Dystroglycan-IR. Fig 6A is a cross-section of the crista ampullaris, close to the central zone. α-dystroglycan-IR (red color) was seen within the BMs underneath the sensory epithelia (SE) (double arrows). In comparison to the BM proteins, collagen IV and laminin-β2, the α-dystroglycan-IR was relatively less intense at the lateral and basal zone of the crista ampullaris (single arrow), and significantly less prominent within the BMs beneath the TE and within the perivascular BMs. The macula utricle (Fig 6B) and macula saccule (Fig 6C) exhibited a similar α-dystroglycan-IR pattern as the crista ampullaris. α-dystroglycan-IR was noted in BMs underneath the maculae sensory epithelia in close apposition with the basal portion of the supporting cells (arrows). BMs that surround stromal myelinated nerve fibers of the macula utricle and saccule also exhibited α-dystroglycan-IR (thick arrowheads). DAPI (blue color) identifies cell nuclei. Magnification bar is 200 μm for all figures.

NIH-PA Author Manuscript NIH-PA Author Manuscript NIH-PA Author Manuscript

NIH-PA Author Manuscript
NIH-PA Author Manuscript
NIH-PA Author Manuscript

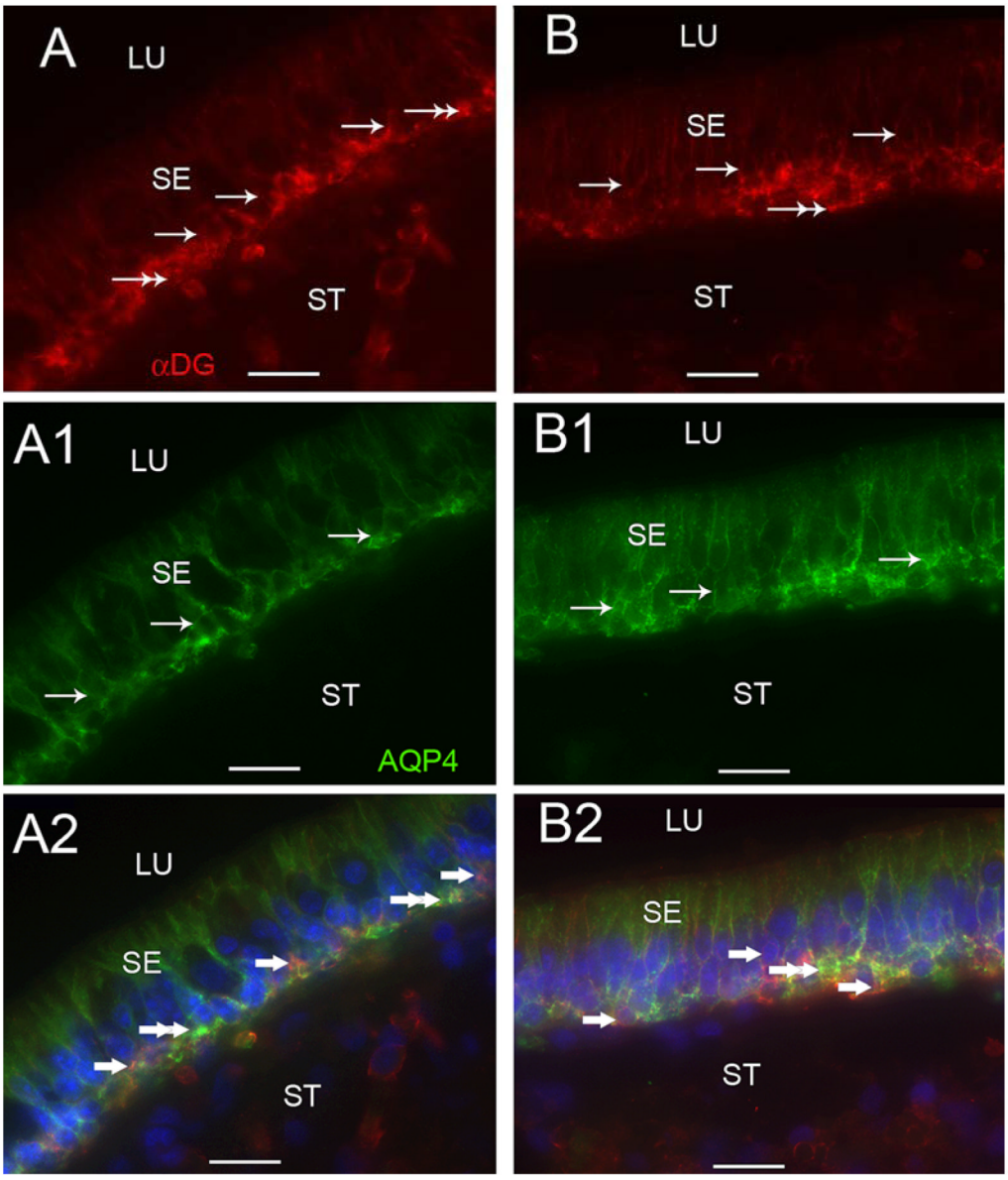

Fig 7.

α-Dystroglycan-IR and AQP4-IR co-distribution in vestibular supporting cells. Fig 7A, 7A1 and 7A2 are cross-sections of the crista ampullaris, near the central region. Fig 7A demonstrates α-dystroglycan-IR (red color) localized to the basal pole of supporting cells (arrows) and to the BM underlying the sensory epithelium (SE) (double arrows). Fig 7A1 demonstrates AQP4 (green color) localization to the basolateral portion of the supporting cells (arrows); the BM underlying the SE and the perineural and perivascular BMs in the stroma (ST) did not exhibit AQP4-IR. Fig 7A2 is a merged image from 7A and 7A1 to illustrate the co-distribution and co-localization of α-dystroglycan and AQP4. α-dystroglycan in red color (arrowheads) segregated to the stromal (ST) perineural BMs and appeared to segregate to portions of the BM underlying the sensory epithelium (SE). AQP4 (green color) appeared to co-localize with α-dystroglycan (red color) with resulting yellow color within the basal supporting cells (double arrowheads). Fig 7B, 7B1 and 7B2 are cross-sections of the macula utricle. Fig 7B demonstrates that αdystroglycan-IR (red color) localized to the basal supporting cells (arrows) and the BM

underlying the SE (double arrows). Fig 7B1 demonstrates that AQP4-IR (green color) localized to basolateral supporting cells (arrows). Fig 7B2 is a merged micrograph demonstrating the co-localization of α-dystroglycan and AQP4 (yellow color at double arrows) in the basolateral aspect of the utricular supporting cells. Magnification bar is 25 μm for all figures.

NIH-PA Author Manuscript
NIH-PA Author Manuscript
NIH-PA Author Manuscript

NIH-PA Author Manuscript
NIH-PA Author Manuscript
NIH-PA Author Manuscript

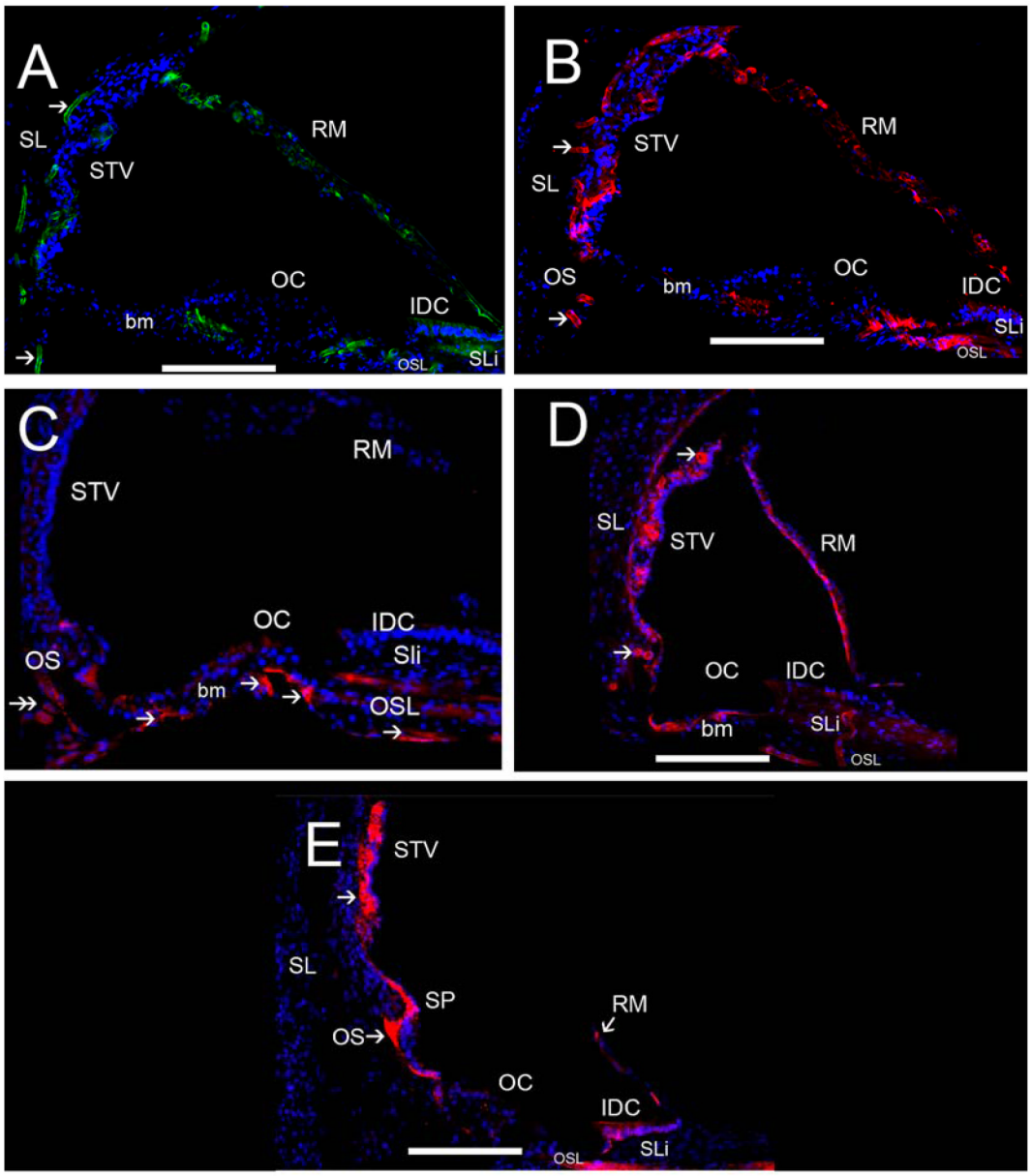

Fig 8.

ECM protein-IR in the human cochlea. Fig 8A exhibits strong collagen IVα2-IR in strial and spiral ligamental perivascular BMs (arrowheads), less intense collagen IVα2-IR was seen at the interdental cells (IDC) and basilar membrane (bm). Collagen IVα2 was expressed in Reissner's membrane (RM). Fig 8B shows strong nidogen-IR in strial and spiral ligamental perivascular BMs (arrowheads), in the IDC, in RM and the osseous spiral lamina (OSL). Fig 8C demonstrates tenascin-C-IR within BMs of the basilar membrane underneath the supporting cells in the pars arcuata (PA) and pars pectinata (PP) and within the OSL (double arrowhead). Tenascin-C-IR was also seen in the basal portion of the Rosenthal canal (RC). Fig 8D shows laminin-β2-IR within most cochlear BMs including the strial and spiral ligamental perivascular BMs (arrows), in RM, and the IDC, and in the basilar membrane. Fig 8E demonstrates α-dystroglycan-IR within most cochlear BMs (arrowheads) with strong IR in cells of the outer sulcus (OS), the IDC, RM, the spiral prominence and stria vascularis perineural BMs. The

NIH-PA Author Manuscript

NIH-PA Author Manuscript

NIH-PA Author Manuscript

inner and outer hair cells and the supporting cells in the organ of Corti (OC) were not reactive for any ECM proteins. All of the basement membrane proteins were expressed to differential degrees within Reissner's membrane, the basilar membrane, and the interdental cells. Perineural and perivascular BMs in the STV and the spiral ligament (SL) expressed collagen α2IV, nidogen and laminin-β2. The tectorial membrane was not visualized because it had become detached during the microdissection of the cochlea. Magnification bar is 100 μm for all figures.

NIH-PA Author Manuscript
NIH-PA Author Manuscript
NIH-PA Author Manuscript

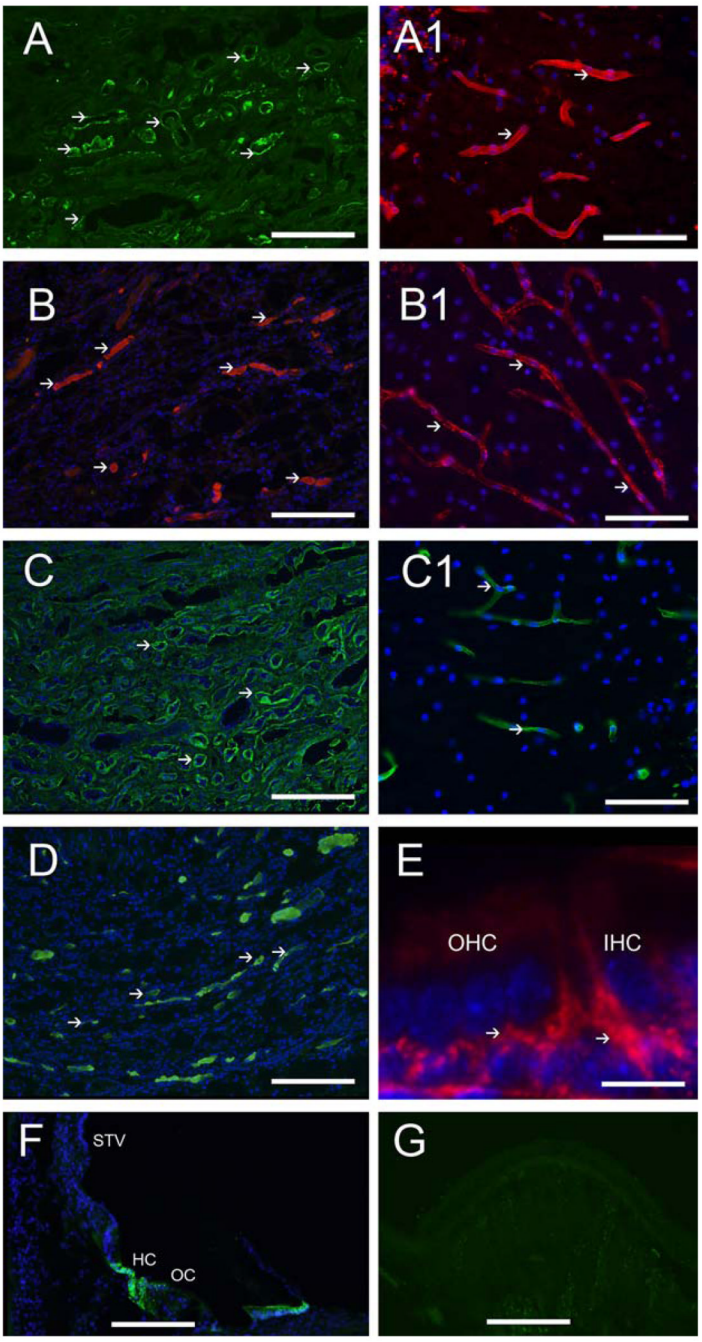

Fig 9.

Positive controls for BM antibodies. Fig 9A shows nidogen-IR in tubular BMs of the human kidney (arrowheads). Fig 9A1 shows nidogen-IR in perivascular BMs of the human cerebral cortex (arrowheads). Fig 9B shows αdystroglycan-IR in tubular BMs of the human kidney (arrowheads). Fig 9B1 shows αdystroglycan-IR in perivascular BMs of the human cerebral cortex (arrowheads). Fig 9C shows collagen IVα2-IR in the human kidney BMs (arrowheads). Fig 9C1 shows collagen IVα2-IR in perivascular BMs of the human cerebellar cortex (arrowheads). Fig 9D shows laminin-β2-IR in BMs of the human kidney (arrowheads). Fig 9E shows tenascin-C-IR underneath the inner and outer hair cells of the one day old mouse (arrowheads). Fig 9F shows AQP4-IR in Hensen cells (HC) of the human organ of Corti (OC).

NIH-PA Author Manuscript

NIH-PA Author Manuscript

NIH-PA Author Manuscript

STV: stria vascularis. Fig 9G demonstrates an example of human crista ampullaris immunostained with all the reagents except for the primary antibody. No specific immunoreaction was observed. Magnification bar is 200 μm for figures A–D, and F and G, 10 μm for E.

NIH-PA Author Manuscript

NIH-PA Author Manuscript

NIH-PA Author Manuscript

Table 1

Postmortem time and quality of immunostaining

Postmortem time/Sex/Age	Crista ampullaris	Utricular macula	Saccular macula	Cochlea
6 hrs/F/85 years	++	++	++	++
5 hrs/F/91 years	++	++	++	++
8 hrs/F/ 86 years	+	+	+	+
4 hrs/F/94 years	+++	+++	+++	+++
3 hrs/M/84 years	+++	+++	+++	+++

Excellent quality: +++ (no background, immunoreactive signal intense)
Good quality: ++ (no background, immunoreactive signal less intense)
Regular quality: + (some background, immunoreactive signal much less intense).
F: female, M: male.

NIH-PA Author Manuscript

NIH-PA Author Manuscript

NIH-PA Author Manuscript

Table 2

Antibodies: source, type, dilution, specificity, immunogen, and controls.

Antibody/ Source/ Cat #	**Antibody type/ dilution**	**Specificity/ Immunogen**	**Positive/ negative controls**
Collagen IVα2/ Chemicon Int./MAB1910	Mouse monoclonal IgG / 1:500	Human type IV collagen α2 chains/ Human amniotic type IV collagen	Human kidney and brain BMs (Fig 9)/ Omission of the antibody (no reaction)
Nidogen-1/ Calbiochem/ 481918	Rabbit polyclonal IgG / 1:500	Human nidogen/ Purified, human placental nidogen.	Human kidney and brain BMs (Fig 9)/ Omission of the antibody (no reaction)
Tenascin-C/ Chemicon Int./ AB19013	Rabbit polyclonal IgG / 1:1000	Tenascin chicken, human and mouse/ Purified tenascin from embryonic chicken brain	Mouse cochlea (Fig 9)/ Omission of the antibody (no reaction)
Laminin-β2/ Upstate/ 05–206	Rat monoclonal IgG / 1:200	Human and mouse β2 chain laminin/ Murine EHS laminin	Human kidney BMs(Fig 9)/ Omission of the antibody (no reaction)
αDystroglycan Upstate/ 05–593	Mouse ascites IgM / 1:250	αDystroglycan from human, mouse, rat/ rabbit skeletal muscle membrane preparation	Human kidney and brain BMs (Fig 9)/ Omission of the antibody (no reaction)
Aquaporin-4/ Santa Cruz/ Sc-20812	Rabbit polyclonal IgG / 1:1000	AQP4 mouse, rat and human/ amino acids 244–323 mapping at the C-terminus of AQP4 of human origin	Human cochlea and brain (Fig 9)/ Omission of the antibody (no reaction)

Chemicon Int. (Temecula, CA); Upstate (Temecula, CA); Calbiochem (La Jolla, CA); Santa Cruz Biotechnology (Santa Cruz, CA)

NIH-PA Author Manuscript

NIH-PA Author Manuscript

NIH-PA Author Manuscript

Table 3

Basement membrane (BM) protein localization in human vestibular endorgans.

Protein	Stroma	Sensory epithelia	Transition epithelia
Collagen IVα2/	PV BM+++ PN BMs++	BM+++	BM+++
Nidogen/	PV BM+++ PN BM+++	BM+++	BM+++
Tenascin-C/	PV BM − PN BM−	Epithelial BM: CA central zone+++ CA peripheral PS zone − MU and MS BMs ++ Type I-Like calyces (CA, MU and MS) +++	BM
Laminin-β-2/	PV BM++ PN BM++	BM++	BM+++
αDystroglycan	PV BM+ PN BM+	BM+++	BM−

Legend: CA cristae ampullares; MU: macula utricle, MS macula saccule; PS planum semilunatum; PV: perivascular; PN: perineural

−= not detected

+= faintly immunoreactive

++= immunoreactive

+++= highly immunoreactive

NIH-PA Author Manuscript
NIH-PA Author Manuscript
NIH-PA Author Manuscript

Table 4

BM protein localization in the human cochlea.

Protein	STV	RM	SL	IDC	OS	IS	bm	Slim	OSL	OC (IHC+OHC)
Collagen IVα2/	PV & PN +++	+++	PV+++	++	++	+	+	++	++	−
Nidogen/	PV & PN +++	+++	PV+++	++	++	+	+	++	+++	−
Tenascin-C/	−	−	−	−	−	−	+++	−	+++	−
Laminin-β-2/	PV & PN +++	+++	PV +++	+	+	+	++	++	+++	−
αDystroglycan	+++	+++	−	+++	+++	++	−	−	+++	−

Legend: OC; Organ of Corti; IHC:inner hair cells; OHC:outer hair cells; STV: stria vascularis; Reissner's membrane: RM; Spiral ligament: SL; Interdental cells IDC; Outer sulcus:OS; Inner sulcus: IC, basilar membrane: bm; Spiral limbus: Slim; Osseous spiral lamina:OSL; PV: perivascular; PN: perineural

−= not detected

+= faintly immunoreactive

++= immunoreactive

+++= highly immunoreactive